GPR87 protects UVB-damaged skin by coordinating antioxidant, DNA repair, and anti-Inflammatory responses via Nrf2 and PI3K/AKT–NF-κB pathways

Kai Zang[1#], Biao Guo[1#], Jia-Hui Yu[1], Ruo-Yun Liu[1], Tang-Lin Liu[1], Cai-Bing Wang[5], Peng Xu[3,4]*, Yong-Yan Dang[1,2]*

[1]Institute of Biomedical Sciences and School of Life Sciences, East China Normal University, Shanghai 200241, China

[2]China Liwa Institute of Skin Health, East China Normal University, Shanghai, 200241, China

[3]Yunnan Botanee Bio-technology Group Co., Ltd., Kunming 650106, China

[4]Yunnan Characteristic Plant Extraction Laboratory, Yunnan Characteristic Plant Extraction Laboratory Co., Ltd., Kunming 650106, China

[5]Shanghai Institute of Nutrition and Health, University of Chinese Academy of Sciences, Chinese Academy of Sciences, Shanghai 200031, China

Co-first author.

*Authors for correspondence:
East China Normal University,
500 Dongchuan Road,
Shanghai 200241
P.R.China
Tel: +86-21-54345482
E-mail: yydang@bio.ecnu.edu.cn

Funding

This work was supported by the National Natural Science Foundation of China (82273072, 81972561).

Science Press
ZR Zoological Research

ABSTRACT

GPR87 has been implicated in tumorigenesis, malignant progression, and remodeling of the tumor microenvironment in various cancers; however, its function in the skin remains largely unexplored, despite its high expression in skins. Interestingly, we found that UVB exposure downregulates GPR87 expression in human skin tissues, HaCaT keratinocytes, and mouse skin. Importantly, loss of GPR87 was shown to exacerbate UVB-induced skin injury in *GPR87*-knockout C57BL/6 mice. In keratinocytes, RNA interference–mediated knockdown of GPR87 resulted in increased reactive oxygen species (ROS) levels. Consistently, both *in vivo* and *in vitro* data showed that GPR87 deficiency enhances inflammatory responses and cyclobutane pyrimidine dimer (CPD) accumulation, while attenuating apoptosis in skin cells. Moreover, GPR87 promotes CPD clearance by regulating the XPC expression and ubiquitination, a key component of the nucleotide excision repair pathway. Mechanistically, GPR87 exerts its antioxidant effects by promoting Nrf2 nuclear translocation and inducing downstream antioxidant gene expression. Loss of GPR87 also activates the PI3K/AKT pathway and its downstream effector NF-κB. Notably, AKT inhibitor effectively reversed the GPR87 deficiency–induced CPD accumulation and inflammatory responses. Collectively, these findings demonstrate that GPR87 protects UVB-damaged skin by coordinating antioxidant, DNA repair, and anti-inflammatory responses via Nrf2 and PI3K/AKT–NF-κB pathways, identifying GPR87 as a key endogenous factor in maintaining skin homeostasis under environmental stress. Thus, targeting GPR87 may represent a promising strategy to prevent or mitigate UVB-induced photodamage and related skin disorders.

Keywords: GPR87; UVB; skin; DNA damage; Nrf2; PI3K/AKT pathway

Science Press ZR Zoological Research

INTRODUCTION

The skin, the body's largest organ, serves as the first line of defense against environmental insults and also contributes to immune surveillance, thermoregulation, and sensory perception(Souto-Silva et al., 2025) . Among environmental stressors, ultraviolet (UV) radiation, especially UVB, is a major factor that disrupts skin homeostasis. Excessive UVB exposure induces oxidative stress and DNA damage, provokes inflammatory responses, accelerates photoaging, and contributes to skin carcinogenesis(Tang et al., 2024; Yang and Lan, 2025). Although certain plant extracts and corticosteroids have been used to alleviate UV-induced skin damage(Huang et al., 2024; Sajeeda et al., 2024), their clinical effectiveness remains limited due to transient effects and the risk of adverse reactions.

The molecular mechanisms underlying UVB-induced skin damage are highly intricate. It is well-established that UVB exposure can trigger the excessive ROS production and cause direct DNA damage, such as the formation of CPDs(Wang et al., 2022). Evidence also indicates that UVB exposure activates multiple signal transduction pathways in epidermal cells, notably the PI3K/AKT, MAPK, and NF-κB pathways(Ansary et al., 2021; Hwang et al., 2020; Xu et al., 2022). It is reported that oxidative stress driven by UV-induced ROS plays a central role in triggering PI3K/AKT signaling, which in turn contributes to the activation of NF-κB(Bang et al., 2021). These pathways regulate the expression of pro-inflammatory cytokines and mediate the skin's inflammatory responses to UV damage. Therefore, persistent oxidative stress can elicit inflammatory responses, which in turn aggravate tissue injury(Jin et al., 2024). Although the AKT, MAPK, and NF-κB pathways play key roles in UVB-induced skin damage, their direct inhibition may disrupt essential physiological processes and lead to undesirable side effects. Thus, it is urgent to identify and validate novel molecular targets in order to develop more effective interventions for UVB-induced skin injury.

G protein–coupled receptors (GPCRs) are a major class of drug targets and account for a substantial proportion of approved therapeutics. In recent years, Increasing evidence also highlights critical roles for GPCRs in skin physiology and pathology, particularly in regulating inflammation, barrier function, and responses to environmental stressors(Wang et al., 2024; Zhang et al., 2024). GPR87, a member of the rhodopsin-like class A GPCR family, has been identified as a receptor for lysophosphatidic acid

Science Press ZR Zoological Research

(LPA)(Geraldo et al., 2021). Mounting evidences implicates GPR87 in the development and progression of various malignancies, including lung, pancreatic, bladder, and hepatocellular cancers(Sak, 2025). According to the Human Protein Atlas, GPR87 exhibits "tissue-enhanced" expression in the skin, implying a specific and potentially significant role in cutaneous biology. However, its functions in normal skin physiology and non-malignant skin disorders remain largely unknown. Given the role of LPA in wound healing, keratinocyte proliferation and skin inflammation(Huang et al., 2025; Kim et al., 2022; Xie et al., 2025), and the fact that UVB-induced skin damage involves both processes, we hypothesize that GPR87 may contribute to the cutaneous response to UVB exposure.

In this study, we established UVB-induced skin damage models using *Gpr87*-knockout mice and *GPR87*-silenced HaCaT keratinocytes to investigate the role and underlying mechanisms of GPR87 in this process. Loss of GPR87 exacerbates UVB-induced skin injury in mice. Moreover, GPR87 deficiency promotes skin inflammation and CPD accumulation, attenuates apoptosis and nucleotide excision repair, mainly likely via Nrf2 inhibition and PI3K/AKT–NF-κB activation. Thus, GPR87 may act as a protective factor and represent a novel therapeutic target for UVB-induced skin damage in the future.

MATERIALS AND METHODS

Cell culture and UVB irradiation

HaCaT (ATCC) cells were cultured in DMEM supplemented with 10% fetal bovine serum (FBS), 100 U/mL penicillin G, and 100 μg/mL streptomycin. For UVB treatment, cells were rinsed with PBS to remove residual culture medium and then irradiated at the indicated UVB dose using a calibrated, sterilized UVB lamp (320 nm). Culture plates were placed in the irradiation chamber, and non-irradiated wells were shielded with aluminum foil. After irradiation, PBS was replaced with fresh medium, and the cells were returned to the incubator for subsequent assays.

UVB-induced mouse skin injury model

GPR87 wild-type (*GPR87*$^{+/+}$) and knockout (*GPR87*$^{-/-}$) C57BL/6 mice were obtained from the Laboratory Animal Center of East China Normal University (China). Primers used for genotyping are shown in Supplemental Table 1. All animal experiments were approved by the Ethics Committee of East China Normal University (m20210703).

Female C57BL/6 mice (6–8 weeks old) were used to establish an acute skin injury

Science Press ZR Zoological Research

model. Dorsal hair was removed using a razor and depilatory cream. After cleaning and drying the skin, mice were rested for 24h before UVB exposure. Under anesthesia, mice were irradiated with a single dose of UVB (100 mJ/cm²), while control mice were shielded with aluminum foil. The dorsal area was monitored daily and photographed.

Slot blot assay for CPD detection

Genomic DNA was extracted from UVB-treated HaCaT cells. Denaturation was performed by boiling DNA in 0.32 M NaOH and 5 mmol/L EDTA for 10 min, followed by neutralization in 1.4 M sodium acetate and 0.6 M ammonium acetate. Samples (100 ng DNA) were transferred to NC membranes using a slot blot manifold. Membranes were air-dried, baked at 80°C for 2 h, blocked in 5% milk, and incubated with anti-CPD primary antibody overnight at 4°C. Secondary antibody incubation was followed by visualization using Odyssey.

Flow cytometric analysis of cell cycle

HaCaT cells were UVB-irradiated and collected by trypsinization. Cells were washed with PBS, fixed in 75% ethanol overnight at 4°C, and rehydrated before staining with 50 μg/mL PI and 100 μg/mL RNase A. DNA content was analyzed by flow cytometry to determine cell cycle distribution. The cell cycle distribution was analyzed using FlowJo, and the percentage of cells in each phase (G_0/G_1 phase, S phase, G_2/M phase) relative to the total number of cells was calculated.

TUNEL assay for apoptosis detection

Apoptotic cells were detected using the TUNEL assay kit (manufacturer) according to the manufacturer's instructions. Nuclei were counterstained with DAPI, and apoptotic signals were visualized under a fluorescence microscope.

Flow cytometry for apoptosis

HaCaT cells were UVB-irradiated, harvested, and stained with Annexin V-FITC and PI using an apoptosis detection kit. Stained cells were analyzed using flow cytometry to quantify early and late apoptotic populations.

Statistical analysis

All data are presented as mean±standard deviation (SD). Statistical significance between groups was determined using Student's *t*-test. A P-value<0.05 was considered statistically significant.

RESULTS

Science Press
ZR Zoological Research

UVB Irradiation Suppresses GPR87 Expression *in vitro* and *in vivo*

It is well known that UVB exposure can disrupt skin architecture and homeostasis, leading to acute damage. GPR87, an orphan G protein–coupled receptor belonging to the rhodopsin-like family, is highly expressed in the skin, suggesting its involvement in maintaining skin homeostasis. Bioinformatic analysis of a public transcriptomic dataset (GSE138800) revealed a negative correlation between UVB exposure and *GPR87* expression in HaCaT keratinocytes (Figure 1A). To experimentally validate this observation, depilated C57BL/6 mice were subjected to a single dorsal UVB irradiation, and Gpr87 expression in the skin was assessed by qPCR and Western blotting. To justify the UVB dose used *in vivo*, we compared skin responses to a single exposure at 50 or 100 mJ/cm². A dose of 50 mJ/cm² produced no obvious skin injury, and histological analysis on day 9 post-irradiation showed no significant change in skin thickness compared with the control. In contrast, 100 mJ/cm² induced clear skin damage, as evidenced by a marked increase in skin thickness (Supplemental Figure 1A, 1B). Therefore, we finally selected 100 mJ/cm² as the UVB dose for the animal experiments. Interestingly, the results showed that UVB significantly downregulated Gpr87 expression in mouse skin at both the mRNA and protein levels (Figure 1B, 1C). Consistent with the *in vivo* findings, UVB irradiation of human HaCaT keratinocytes also resulted in a dose-dependent (Figure 1D, 1E) and time-dependent (Figure 1F, 1G) decrease in GPR87 expression. Together, these results demonstrate that UVB irradiation can markedly suppress GPR87 expression in the skin, suggesting a role for GPR87 in skin homeostasis and recovery from UVB-induced damage.

Gpr87 deletion exacerbates UVB-induced acute skin injury in mice

To further elucidate the role of GPR87 in UVB-induced skin injury, we used Gpr87 knockout ($Gpr87^{-/-}$) mice (Supplemental Figure 1C) to establish an acute UVB-induced skin damage model. qPCR results showed that GPR87 was not detected in the skin tissues of *Gpr87* knockout mice, confirming the successful gene deletion (Supplemental Figure 1D). Following dorsal hair removal, mice were exposed to a single dose of UVB irradiation (100 mJ/cm²) (Supplemental Figure 1E). By day 3 post-irradiation, wildtype ($Gpr87^{+/+}$) mice exhibited only mild erythema and scaling, whereas $Gpr87^{-/-}$ mice developed significantly more severe skin damage, including ulceration (Figure 2A). H&E staining showed that Gpr87 deficiency did not affect normal skin architecture. However, by day 3 post-UVB exposure, $Gpr87^{-/-}$ mice

exhibited pronounced epidermal disruption, obscured dermo-epidermal junctions, loss of epidermal layers, and increased inflammatory cell infiltration compared with *Gpr87*$^{+/+}$ mice (Figure 2B). By day 14, *Gpr87*$^{+/+}$ skin had largely recovered, whereas *Gpr87*$^{-/-}$ mice continued to exhibit prominent lesions and significantly increased epidermal thickening (Figure 2C; Supplemental Figure 1F; n=6; $p<0.0001$), indicative of a sustained and heightened inflammatory responses. In addition, Masson's trichrome staining revealed aggravated epidermal injury and reduced, disorganized dermal collagen in *Gpr87*$^{-/-}$ mice after UVB exposure (Supplemental Figure 1G), supporting a more severe skin-damage phenotype. These findings demonstrate that Gpr87 deficiency markedly exacerbates UVB-induced skin injury in mice, indicating that GPR87 may serve as a protective factor in the skin by promoting repair after UVB exposure.

GPR87 deficiency elevates UVB-induced oxidative stress and aggravates inflammatory responses

Upon UVB exposure, excessive ROS are generated in epidermal keratinocytes, causing oxidative stress and contributing to UVB-induced skin injury. Therefore, we investigated whether the protective role of GPR87 involves modulation of ROS generation or downstream oxidative-stress pathways. To this end, we constructed shRNA plasmids targeting GPR87 (sh*GPR87*) and a scramble control (shNC) using lentiviral vectors. HaCaT cells were transduced, GFP-sorted, and assessed for *GPR87* knockdown. As shown in Supplemental Figures 2A and 2B, GPR87 expression was significantly reduced in HaCaT cells following RNA interference. Moreover, UVB irradiation markedly increased ROS levels in HaCaT cells, and this effect was further amplified by *GPR87* knockdown (Figure 3A,3B). Given the central role of Nrf2 in oxidative stress responses, we subsequently assessed whether GPR87 modulates Nrf2 activity. As expected, UVB exposure induced nuclear translocation of Nrf2 in normal cells; however, this process was significantly impaired by *GPR87* knockdown (Figure 3C). Consistently, the expression of Nrf2 downstream antioxidant genes, HO-1 and NQO1， was also markedly reduced following *GPR87* silencing (Figure 3D). These results suggest that the loss of GPR87 impairs the antioxidant capacity of skin cells, thereby exacerbating oxidative damage. PKC is a well-recognized upstream mediator of GPCR-driven Nrf2 activation(Yang et al., 2025), and GPR87 mainly signals via Gq, a pathway capable of engaging PKC. We therefore tested whether PKC is involved in GPR87-mediated Nrf2 activation. In control cells with intact GPR87 expression, UVB robustly induced the Nrf2 target genes HO-1 and NQO1 (Supplemental Figure 3A).

However, the PKC inhibitor GF109203X markedly attenuated this UVB-induced upregulation, reducing HO-1 and NQO1 expression to levels comparable to those in sh*GPR87* cells (Supplemental Figure 3A). These data suggest that GPR87-mediated Nrf2 activation is, at least in part, PKC-dependent.

To corroborate our *in vitro* findings, we further assessed oxidative stress in UVB-irradiated WT and *Gpr87*-KO mice. Biochemical analyses of skin homogenates demonstrated that UVB exposure resulted in a greater increase in malondialdehyde (MDA) (Supplemental Figure 3B) and a more pronounced decrease in superoxide dismutase (SOD) activity (Supplemental Figure 3C) in *Gpr87*-KO mice compared with WT mice. Consistently, immunofluorescence staining of skin sections showed significantly reduced NQO1-positive staining in *Gpr87*-KO mice relative to WT controls after UVB irradiation (Supplemental Figure 3D). Collectively, these data support that GPR87 loss amplifies UVB-induced oxidative stress *in vivo*.

Given that excessive ROS can amplify inflammatory responses, we further assessed the expression of key inflammatory markers. *In vitro*, *GPR87* knockdown significantly upregulated the mRNA expression of pro-inflammatory cytokines, including *IL-6*, *TNF-α*, *CXCL1*, *CXCL8*, and *CCL20*, and also markedly increased the transcription and translation of COX-2 (Figure 4A, 4B). *In vivo*, UVB-treated *Gpr87*$^{-/-}$ mice exhibited enhanced dermal infiltration of F4/80^{+} macrophages (Figure 4C, 4D; n=6, p= 0.0002), accompanied by markedly higher expression of *IL-6*, *TNF-α*, and *CXCL1* in the epidermis (Figure 4E). Collectively, these findings suggest that GPR87 deficiency impairs ROS clearance following UVB exposure, thereby triggering excessive inflammatory responses.

GPR87 deficiency exacerbates UVB-induced DNA damage

Cyclobutane-pyrimidine dimers (CPDs), one of the most critical forms of DNA damage, are rapidly formed in the skin within minutes of UVB exposure. Therefore, we investigated whether GPR87 deficiency affects the accumulation of UVB-induced CPDs using immunofluorescence staining. In HaCaT cells, UVB exposure induced CPD formation compared to the control; notably, the number of CPD-positive cells was significantly increased upon GPR87 knockdown (Figure 5A, 5B). Meanwhile, slot blot assays further confirmed delayed CPD repair kinetics in GPR87-deficient cells (Figure 5C, 5D). Immunofluorescence analysis of mouse skin further demonstrated

increased CPD accumulation in the epidermis of *Gpr87*$^{-/-}$ mice compared with *Gpr87*$^{+/+}$ mice following UVB irradiation (Figure 5E, 5F; n=6, p=0.0007). These results indicate that GPR87 deficiency increases the accumulation of UVB-induced CPDs in both human keratinocytes and mouse epidermis, thereby exacerbating UVB-induced skin damage.

GPR87 deficiency impairs UVB-induced DNA damage repair

CPDs are primarily removed through the global genome nucleotide excision repair (GG-NER) pathway. XPC plays a crucial role in the initial recognition of UVB-induced DNA damage, serving as a key sensor that detects helical distortions and initiates repair. As expected, UV irradiation triggered a rapid increase in XPC ubiquitination, promoting efficient recognition of damaged DNA (Figure 6A). Notably, this UV-induced XPC ubiquitination was markedly attenuated in GPR87-knockdown cells compared to the control (Figure 6A, 6B), suggesting that GPR87 is required for efficient DNA damage recognition. To further validate the role of GPR87 in regulating XPC ubiquitination, we conducted proteasomal inhibition assays using MG132. Blocking proteasomal activity largely rescued the diminished ubiquitinated XPC signal in *GPR87*-knockdown cells (Supplementary Figure 4A). These results further support that GPR87 modulates UVB-triggered XPC ubiquitination. We next investigate whether GPR87 deficiency affects the expression of key GG-NER proteins, including XPA, XPB, and XPC (Figure 6C). In HaCaT cells with intact GPR87, XPC levels showed a transient decrease at 3h after UVB irradiation and recovered by 6h. In contrast, XPC levels remained low in *GPR87*-knockdown cells (Figure 6B, 6C), suggesting impaired restoration of XPC expression after UVB exposure. This observation was further supported by qPCR analysis of XPC mRNA, which revealed a similar trend (Figure 6D). In mouse skin, both qPCR and Western blot analyses showed that UVB exposure led to a significantly lower level of XPC expression in *Gpr87*$^{-/-}$ mice compared to *Gpr87*$^{+/+}$ controls, further supporting a role for GPR87 in maintaining XPC levels (Figure 6E, 6F; Supplemental Figure 4B). Moreover, in sh*GPR87* cells, the expression of XPA was reduced in response to UVB irradiation, while XPB levels remained unchanged (Figure 6C). Consistently, the DNA damage marker γH2AX was markedly elevated in *GPR87*-knockdown cells compared to control cells (Figure 6C, 6F). These results suggests that the absence of GPR87 hinders the proper repair of DNA damage.

Science Press ZR Zoological Research

CHK1 and CHK2 are key checkpoint kinases that induce cell cycle arrest or delay, thereby providing time for DNA repair. In normal HaCaT cells, UVB treatment increased the phosphorylation of ATR, ATM, CHK1, and CHK2. However, this phosphorylation was significantly reduced in sh*GPR87* cells (Figure 6G), indicating impaired activation of the DNA damage checkpoint response. p53 acts as the 'guardian of the cell cycle' by sensing DNA damage and inducing cell cycle arrest at both the G1/S and G2/M checkpoints. Notably, p53 levels were also markedly reduced in *GPR87*-deficient cells (Figure 6G). Thus, checkpoint deficiency induced by *GPR87* knockdown may be related to impaired p53–dependent cell-cycle arrest. Flow cytometry analysis further confirmed that UVB-treated control cells underwent arrest in both G1 and G2 phases, whereas sh*GPR87* cells failed to initiate this checkpoint response (Figure 6H, 6I; Supplemental Figure 4C). Thus, GPR87 is required for proper DNA damage repair responses and cell-cycle checkpoint activation, likely via the ATR/CHK1 and ATM/CHK2 pathways.

Overall, all the data suggest that deletion of *GPR87* gene impairs the recognition and repair of UVB-induced DNA damage in skin keratinocytes, thereby leading to the accumulation of CPDs.

GPR87 deficiency inhibits apoptosis in UVB-damaged skin keratinocytes

In addition to removing DNA lesions via the NER pathway, skin cells also eliminate irreparably damaged cells through apoptosis, thereby preventing the fixation of UVB-induced CPDs into mutations. As expected, TUNEL assays in HaCaT cells revealed a time-dependent increase in apoptosis following UVB exposure in control cells, whereas significantly fewer apoptotic cells were observed in the *GPR87* knockdown groups (Figure 7A, 7B). This trend was further confirmed by flow cytometry analysis (Supplemental Figure 5A). Western blot results showed that *GPR87* knockdown attenuated the UVB-induced upregulation of the pro-apoptotic factor Bax and downregulation of the anti-apoptotic factor Bcl-2 (Figure 7C). *In vivo*, $Gpr87^{-/-}$ mice exhibited fewer TUNEL-positive epidermal cells compared to $Gpr87^{+/+}$ mice following UVB exposure (Figure 7D, 7E; n=6; p=0.0028), consistent with the in vitro findings. In addition, Western blot analysis revealed a reduced Bax/Bcl-2 ratio in $Gpr87^{-/-}$ mice (Figure 7F). To further characterize the apoptotic pathway affected by GPR87 under UVB stress, we examined caspase-8 activation and PARP cleavage by Western blotting. UVB-induced cleavage of caspase-8 and PARP was reduced in *GPR87*-knockdown

cells compared with control cells (Supplementary Figure 5B, 5C), indicating attenuated apoptotic signaling upon GPR87 depletion. These results suggest that GPR87 deficiency mitigates apoptosis in response to UVB-induced damage.

GPR87 deficiency promotes the activation of PI3K/AKT–NF-κB signal pathway

Substantial evidence has confirmed that the phosphatidylinositol 3-kinase (PI3K)/AKT and NF-κB pathways are among the most critical signaling cascades activated by UV exposure, contributing to DNA damage repair, inflammation, and apoptosis. As expected, UVB exposure in HaCaT cells increased p110α expression and AKT phosphorylation at Ser473, confirming the activation of the PI3K/AKT and NF-κB signaling pathways (Figure 8A). Notably, *GPR87* knockdown further enhanced p110α expression and AKT phosphorylation. PTEN is a negative regulator of the PI3K/AKT pathway, and *GPR87* knockdown reduced PTEN expression at both the mRNA and protein levels in HaCaT cells (Figure 8A; Supplemental Figure 6A). Consistently, UVB-induced AKT phosphorylation (Ser473) was increased in the skin of *Gpr87*$^{-/-}$ mice, in line with the *in vitro* results (Figure 8B). Meanwhile, we also found that UVB exposure increased the phosphorylation of IKKα/β (Ser176/180) and p65 (Ser536), indicating activation of the NF-κB pathway both *in vitro* and *in vivo* (Figure 8B, 8C). Interestingly, LY294002 markedly suppressed UVB-induced p65 phosphorylation in both shNC and sh*GPR87* cells (Figure 8D), suggesting that NF-κB activation may occur downstream of AKT under UV stress. Given the potential off-target effects of LY294002, we validated this with the AKT inhibitor MK-2206, which attenuated the heightened UVB-induced expression of *TNFα*, *CCL20*, and *CXCL1* in *GPR87*-knockdown cells (Supplemental Figure 6B). Together, these data support that GPR87 loss enhances the activation of UVB-induced PI3K/AKT and its downstream NF-κB signaling pathways.

GPR87 deficiency enhances UVB-induced ROS generation, CPD accumulation, inflammation, and apoptosis via the PI3K/AKT pathway

To determine whether the exacerbated skin damage caused by GPR87 deficiency is dependent on the PI3K/AKT signaling pathway, we treated HaCaT cells with the PI3K inhibitor LY294002 in combination with UVB. Although sh*GPR87* cells displayed higher levels of inflammatory cytokines (TNF-α, CXCL1, and CCL20) than control cells after UVB irradiation, this increase was abolished by LY294002 treatment (Figure

8E). Additionally, LY294002 treatment reduced CPD accumulation in UVB-irradiated sh*GPR87* cells from 13.1% to 5.12%, a level comparable to that of control cells (Figure 8F; Supplemental Figure 6C). LY294002 also increased apoptosis in both cell types (shNC: 13.38% → 22.69%; shGPR87: 5.57% → 19.12%), eliminating the survival advantage in GPR87-deficient cells (Figure8F; Supplemental Figure 6D). Together, these findings illustrate that GPR87 loss promotes excessive UVB-induced inflammation, impaired DNA repair, and reduced apoptosis through overactivation of the PI3K/AKT–NF-κB axis, ultimately exacerbating acute skin damage.

DISCUSSION

UVB-induced skin damage is a multifaceted process involving oxidative stress, DNA damage, inflammation, apoptosis, barrier disruption, and immune dysregulation(Zhao et al., 2025). Given the complexity of both the injury and subsequent repair responses, the molecular mechanisms remain to be elucidated to achieve a more complete understanding of UVB-induced cutaneous pathology. In this study, we show for the first time in a murine UVB-injury model that GPR87 deficiency worsens UVB-induced skin damage. Loss of GPR87 enhances inflammation and increases CPD accumulation. Mechanistically, GPR87 is required for proper XPC expression and ubiquitination, supporting nucleotide excision repair. Moreover, GPR87 loss reduces ROS clearance by suppressing the Nrf2 pathway, which in turn activates PI3K/AKT and NF-κB signaling and further amplifies inflammation and DNA damage. Together, these findings uncover a previously unrecognized protective role of GPR87 in maintaining cutaneous homeostasis under UVB stress.

GPR87 has previously been studied primarily in the contexts of cancer and inflammation(Bai et al., 2022; Zhu et al., 2025); however, its new physiological roles remain unclear. The consistent downregulation of GPR87 expression in human skin, HaCaT keratinocytes, and mouse skin afer UVB exposure suggests that GPR87 may be a key endogenous factor in maintaining skin homeostasis under environmental stress. Importantly, both genetic ablation of GPR87 in mice and RNA interference-mediated knockdown in keratinocytes led to exacerbated skin cell injury, highlighting its protective function. Thus, targeting GPR87 or its downstream signaling pathways may represent a novel strategy for preventing or mitigating photodamage and related skin disorders. However, the mechanisms by which UVB downregulates GPR87 remain unclear. We speculate that UVB-induced oxidative stress and DNA damage may

suppress GPR87 via transcriptional repression or epigenetic regulation. Future studies will examine GPR87 promoter methylation and perform ChIP-based analyses to clarify this regulation.

UVB irradiation can damage mitochondrial membrane and increase ROS production, which drives skin inflammation and DNA damage. Interestingly, we found that GPR87 deficiency further enhances UVB-induced ROS accumulation in skin cells, indicating more severe oxidative stress. Moreover, GPR87 exerts its antioxidant function by suppressing Nrf2 nuclear translocation and its transcriptional activation of downstream genes such as HO-1 and NQO1. Previous studies have shown that GPR30 is also downregulated by UVB irradiation in epidermal stem cells and possesses antioxidant and anti-inflammatory functions(Zhang et al., 2019). This is consistent with our findings and suggests an important role for GPCRs in maintaining skin homeostasis. In addition, it is reported that Evidence suggests that PKC, including PKCδ, can promote NRF2 activation under oxidative stress (Yang et al., 2025) . GPR87 is involved in various ligand-mediated signaling pathways, including the PLC/PKC and MAPK pathways(Ma et al., 2020). Thus, we speculate that GPR87 is required for Nrf2 activation, potentially via PKC signaling; however, this requires further experimental confirmation.

UVB induces DNA damage, mainly through the formation of CPDs and 6-4PPs, with CPDs being most abundant. Our cell and animal data show that GPR87 deficiency increases CPDs, suggesting impaired CPD clearance. CPD repair mainly depends on the nucleotide excision repair pathway, in which XPC ubiquitination is essential for damage recognition(Xu et al., 2025). We found that GPR87 deficiency reduces XPC ubiquitination and prevents XPC upregulation after UVB exposure, suggesting that GPR87 may support UVB-induced DNA repair by regulating XPC. In contrast, basal XPC levels were similar between control and GPR87-deficient cells, indicating that GPR87 mainly functions in the UVB-triggered DNA damage response.

It is reported that PTEN downregulation impairs global genomic nucleotide excision repair by suppressing XPC expression via the AKT signaling pathway(Ming et al., 2011). Interestingly, our findings reveal that GPR87 can modulate the PTEN–AKT signaling axis in HaCaT cells and mouse skins in response to UVB irradiation. Loss of GPR87 leads to decreased PTEN expression and enhanced AKT activation, resulting in reduced XPC expression. It is worth noting that GPR87 knockdown reduced PTEN

mRNA levels in HaCaT cells, supporting transcriptional regulation of PTEN by GPR87. The precise mechanism underlying this regulation remains to be defined and will be addressed in future studies using ChIP-based profiling. Moreover, AKT hyperactivation may weaken cell-cycle checkpoints by suppressing key checkpoint regulators, such as the MDM2–p53 axis involved in p53-dependent cell-cycle arrest(Fulcher et al., 2025), thereby reducing the time available for DNA repair and potentially promoting CPD accumulation. Notably, an AKT inhibitor rescued the increased CPDs caused by GPR87 deficiency, suggesting that GPR87 promotes UVB-induced CPD clearance by modulating the PTEN–PI3K–AKT pathway.

UVB is also known to activate NF-κB by inducing IKK-mediated IκBα degradation and subsequent NF-κB translocation to the nucleus (Guo et al., 2024). We found that GPR87 deficiency markedly enhanced UVB-induced phosphorylation of IKKα and p65 in epidermal keratinocytes and increased inflammatory cytokine levels in cells and mouse skin. Importantly, AKT inhibition reduced p-AKT and p-p65 and reversed the elevated UVB-induced inflammatory cytokine expression in *GPR87*-knockdown cells, suggesting that GPR87 regulates NF-κB through the PI3K–AKT pathway. Collectively, these data indicate that the heightened inflammatory infiltration and inflammation in GPR87-deficient skin are mediated, at least in part, by the PI3K–AKT–NF-κB axis.

Apoptosis plays a critical role in eliminating damaged cells and preventing malignant transformation(Tang et al., 2021). GPR87 deficiency reduced UVB-induced apoptosis in keratinocytes and mouse skin, as shown by fewer apoptotic cells and a lower bax/bcl-2 ratio. Thus, the loss of GPR87 may confer resistance to apoptosis in some keratinocytes, potentially increasing the risk of progression to precancerous lesions. Accordingly, elevated CPD and ROS accumulation also indicates a higher susceptibility to UVB-induced skin carcinogenesis over time. These findings suggest that GPR87 may exert a suppressive role in UVB-induced skin carcinogenesis, which warrants further investigation. However, previous studies have shown that GPR87 is upregulated in various cancers, including lung, pancreatic, and liver cancers, where it promotes cell proliferation and migration. We speculate that this tissue-specific functional difference may be related to the skin's chronic exposure to external physical and chemical stressors.

In summary, GPR87 is a novel and critical protective factor in skin repair following UV-induced damage. It suppresses UVB-induced ROS production by activating the Nrf2 pathway, facilitates the clearance of CPD lesions by enhancing XPC expression

and ubiquitination through inhibition of the PTEN–PI3K–AKT signaling cascade, and attenuates excessive inflammatory responses by suppressing the downstream NF-κB pathway. By coordinating antioxidant defenses, inflammatory restraint, and DNA repair, GPR87 mitigates UVB-induced skin damage via the ROS–PI3K–AKT–NF-κB signaling cascades (Supplemental Figure 7). These findings suggest that GPR87 may serve as a promising therapeutic target for the treatment of UVB-induced skin damage, photoaging, and potentially skin carcinogenesis.

COMPETING INTERESTS

The authors declare that they have no conflict of interest.

AUTHORS' CONTRIBUTIONS

K.Z.: Formal analysis, Visualization, Investigation, Methodology and Data Curation; B.G.: Methodology, Validation, Data Curation and Investigation; J.H.Y.: Methodology, Data Curation and Software; R.Y.L.: Software and Investigation; T.L.L.: Methodology and Investigation; C.B.W.: Investigation; P.X.: Formal Analysis; Y.Y.D.: Conceptualization, Funding Acquisition, Resources, Supervision, and Writing - Review & Editing. All authors have read and approved the final version of the manuscript.

FUNDING

This work was supported by the National Natural Science Foundation of China (82273072, 81972561).

REFERENCES

Ansary TM, Hossain MR, Kamiya K, et al. 2021. Inflammatory Molecules Associated with Ultraviolet Radiation-Mediated Skin Aging. *International journal of molecular sciences*, **22**(8). DOI: 10.3390/ijms22083974

Bai R, Zhang JG, He FJ, et al. 2022. GPR87 promotes tumor cell invasion and mediates the immunogenomic landscape of lung adenocarcinoma. *Communications biology*, **5**(1): 663. DOI: 10.1038/s42003-022-03506-6

Bang E, Kim DH, Chung HY. 2021. Protease-activated receptor 2 induces ROS-mediated inflammation through Akt-mediated NF-κB and FoxO6 modulation during skin photoaging. *Redox biology* , **44**: 102022. DOI: 10.1016/j.redox.2021.102022

Fulcher LJ, Sobajima T, Batley C, et al. 2025. MDM2 functions as a timer reporting the length of mitosis. *Nature cell biology,* **27**(2): 262–272.

Geraldo LHM, Spohr T, Amaral RFD, et al. 2021. Role of lysophosphatidic acid and its receptors in health and disease: novel therapeutic strategies. *Signal transduction and targeted therapy*, **6**(1): 45. DOI:

10.1038/s41392-020-00367-5
Guo Q, Jin YZ, Chen XY, et al. 2024. NF-κB in biology and targeted therapy: new insights and translational implications. *Signal transduction and targeted therapy,* **9**(1): 53. DOI: 10.1038/s41392-024-01757-9
Huang F, Liu Q, Lu YN. 2024. Magnolia biondii flower extract attenuates UVB-induced skin damage through high-mobility group box protein B1. *International journal of cosmetic science*, **46**(5): 775–785.
Huang XQ, Lu JHW, An YM, et al. 2025. Electrospun PLGA/PCL Nanofiber Film Loaded with LPA Promotes Full-Layer Wound Healing by Regulating the Keratinocyte Pyroptosis. *ACS applied materials & interfaces*, **17**(14): 20756–20767.
Hwang SY, Chae JI, Kwak AW, et al. 2020. Alternative Options for Skin Cancer Therapy via Regulation of AKT and Related Signaling Pathways. *International journal of molecular sciences*, **21**(18). DOI: 10.3390/ijms21186869
Jin P, Feng XD, Huang CS, et al. 2024. Oxidative stress and cellular senescence: Roles in tumor progression and therapeutic opportunities. *MedComm – Oncology*. DOI:10.1002/mog2.70007
Kim D, Khin PP, Lim OK, et al. 2022. LPA/LPAR1 signaling induces PGAM1 expression via AKT/mTOR/HIF-1α pathway and increases aerobic glycolysis, contributing to keratinocyte proliferation. *Life sciences*, **311**(Pt B): 121201. DOI: 10.1016/j.lfs.2022.121201
Ma S, Yeom J, Lim YH. 2020. Exogenous NAD(+) Stimulates MUC2 Expression in LS 174T Goblet Cells via the PLC-Delta/PTGES/PKC-Delta/ERK/CREB Signaling Pathway. *Biomolecules*, **10**(4). DOI: 10.3390/biom10040580
Ming M, Feng L, Shea CR, et al. 2011. PTEN positively regulates UVB-induced DNA damage repair. *Cancer research*, **71**(15): 5287–5295.
Sajeeda A, Bhat AM, Gorke S, et al. 2024. Naringenin, a flavanone constituent from Sea buckthorn pulp extract, prevents ultraviolet (UV)-B radiation-induced skin damage via alleviation of impaired mitochondrial dynamics mediated inflammation in human dermal fibroblasts and Balb/c mice models. *Journal of photochemistry and photobiology. B, Biology*, **256**: 112944. DOI: 10.1016/j.jphotobiol.2024.112944
Sak K. 2025. The path of GPR87: from a P2Y-like receptor to its role in cancer progression. *Naunyn-Schmiedeberg's archives of pharmacology,* **398**(5): 4803–4815.
Souto-Silva MV, Bispo ECI, De Oliveira NN, et al. 2025. The cytokine-skin barrier axis in health and disease. *Cytokine & growth factor reviews*, **87**: 113–123.
Tang XY, Yang TY, Yu DJ, et al. 2024. Current insights and future perspectives of ultraviolet radiation (UV) exposure: Friends and foes to the skin and beyond the skin. *Environment international*, **185**: 108535. DOI: 10.1016/j.envint.2024.108535
Tang ZT, Tong XL, Huang JH, et al. 2021. Research progress of keratinocyte-programmed cell death in UV-induced Skin photodamage. *Photodermatology, photoimmunology & photomedicine*, **37**(5): 442–448.
Wang M, Zan T, Fan CG, et al. 2024. Advances in GPCR-targeted drug development in dermatology. *Trends in pharmacological sciences*, **45**(8): 678–690.
Wang ZY, Li ZY, Lei YL, et al. 2022. Recombinant Photolyase-Thymine Alleviated UVB-Induced Photodamage in Mice by Repairing CPD Photoproducts and Ameliorating Oxidative Stress. *Antioxidants*, **11**(12). DOI: 10.3390/antiox11122312
Xie XX, Sun JD, Zang MX, et al. 2025. LPA reduces the apoptosis of cryopreserved porcine skin-derived stem cells by inhibiting the regulatory factor TNF-α. *Cryobiology*, **118**: 105189. DOI:

10.1016/j.cryobiol.2024.105189
Xu DF, Li CH, Zhao MM. 2022. Attenuation of UV-induced skin photoaging in rats by walnut protein hydrolysates is linked to the modulation of MAPK/AP-1 and TGF-β/Smad signaling pathways. *Food & function*, **13**(2): 609–623.
Xu P, Liu TL, Yang ZL, et al. 2025. P2RY6 deletion promotes UVB-induced skin carcinogenesis by activating the PI3K/AKT signal pathway. *Cancer science*, **116**(1): 56–66.
Yang TT & Lan CE. 2025. Photocarcinogenesis of the skin: Current status and future trends. *The Kaohsiung journal of medical sciences*, **41**(4): e12946. DOI: 10.1002/kjm2.12946
Yang XY, Liu YC, Cao JH, et al. 2025. Targeting epigenetic and post-translational modifications of NRF2: key regulatory factors in disease treatment. *Cell death discovery*, **11**(1): 189. DOI: 10.1038/s41420-025-02491-z
Zhang YQ, Li L, Xu YC, et al. 2019. Protective mechanism of GPR30 agonist G1 against ultraviolet B-induced injury in epidermal stem cells. *Artificial cells, nanomedicine, and biotechnology*, **47**(1): 4165–4171.
Zhang ZL, Ma XQ, Zhang ZT, et al. 2024. The landscape of GPCR in the skin epidermal stem cells: From the basic to the clinical. *Sheng li xue bao : [Acta physiologica Sinica]*, **76**(6): 881–892.
Zhao CH, Wu SY, Wang H. 2025. Medicinal Plant Extracts Targeting UV-Induced Skin Damage: Molecular Mechanisms and Therapeutic Potential. *International journal of molecular sciences*, **26**(5). DOI: 10.3390/ijms26052278
Zhu DY, Liu DL, Wu K, et al. 2025. GPR87 Promotes Angiogenesis in Esophageal Squamous Cell Carcinoma via VEGFA Regulation. *Molecular carcinogenesis*, **64**(6): 1057–1065.

Science Press
ZR Zoological Research

FIGURE LEGENDS

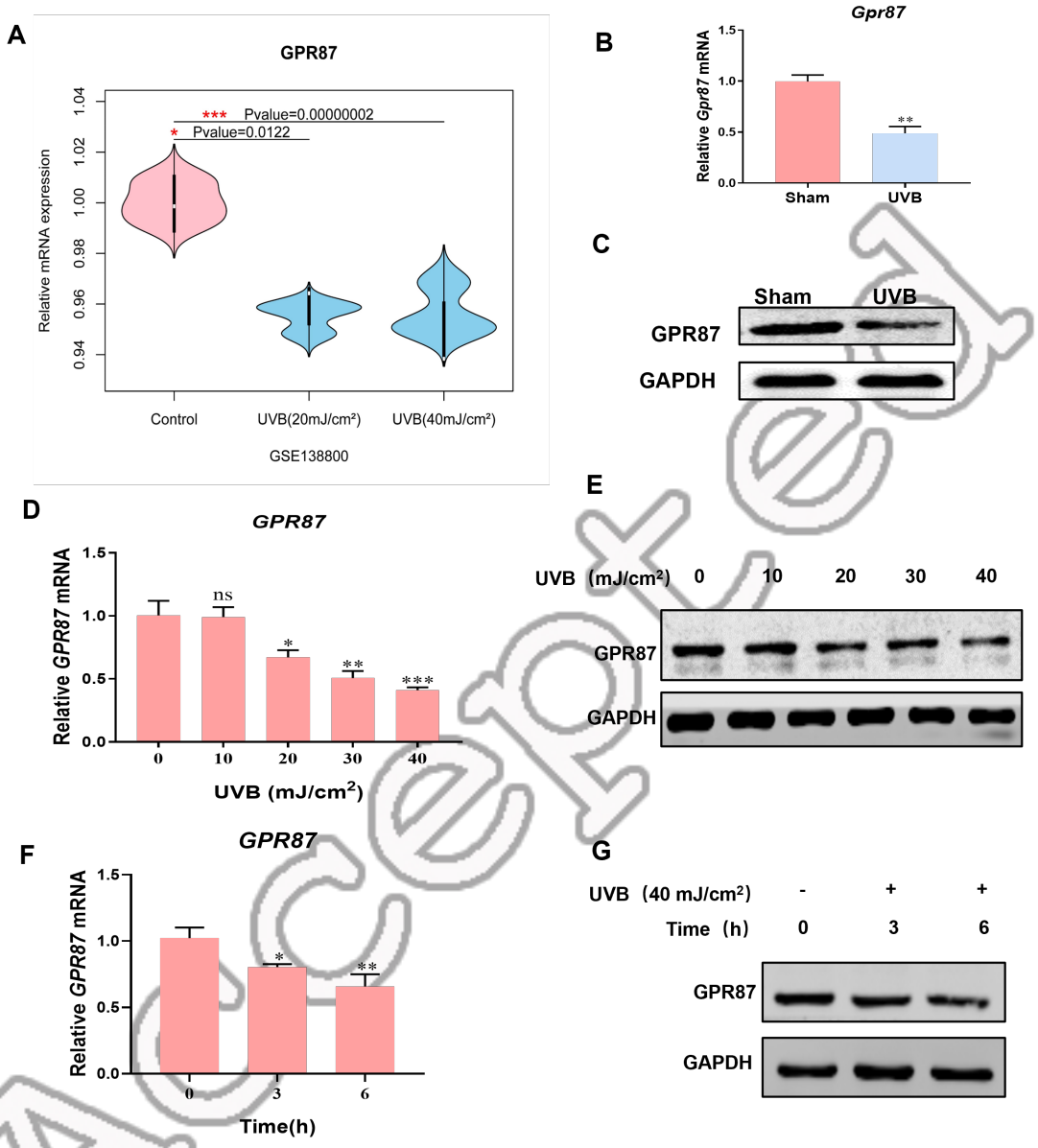

Figure 1. UVB irradiation suppresses GPR87 expression *in vitro* and *in vivo*

A. Bioinformatic analysis of a public transcriptomic dataset (GSE138800) revealed a negative correlation between UVB exposure and GPR87 expression in HaCaT keratinocytes. **B&C.** UVB-induced changes in Gpr87 expression in mouse skin were assessed at the mRNA level by qPCR (B) and at the protein level by Western blotting (C). **D&E.** Western blot and qPCR analyses revealed a dose-dependent decrease in GPR87 expression in HaCaT cells at the mRNA (D) and protein (E) levels. **F&G.** UVB irradiation induced a time-dependent alteration of GPR87 expression in HaCaT cells at

Science Press
ZR Zoological Research

the mRNA (F) and protein (G) levels. Data are presented as mean±SD (n=3). ns, not significant, *P<0.05, **P<0.01, and ***P<0.001.

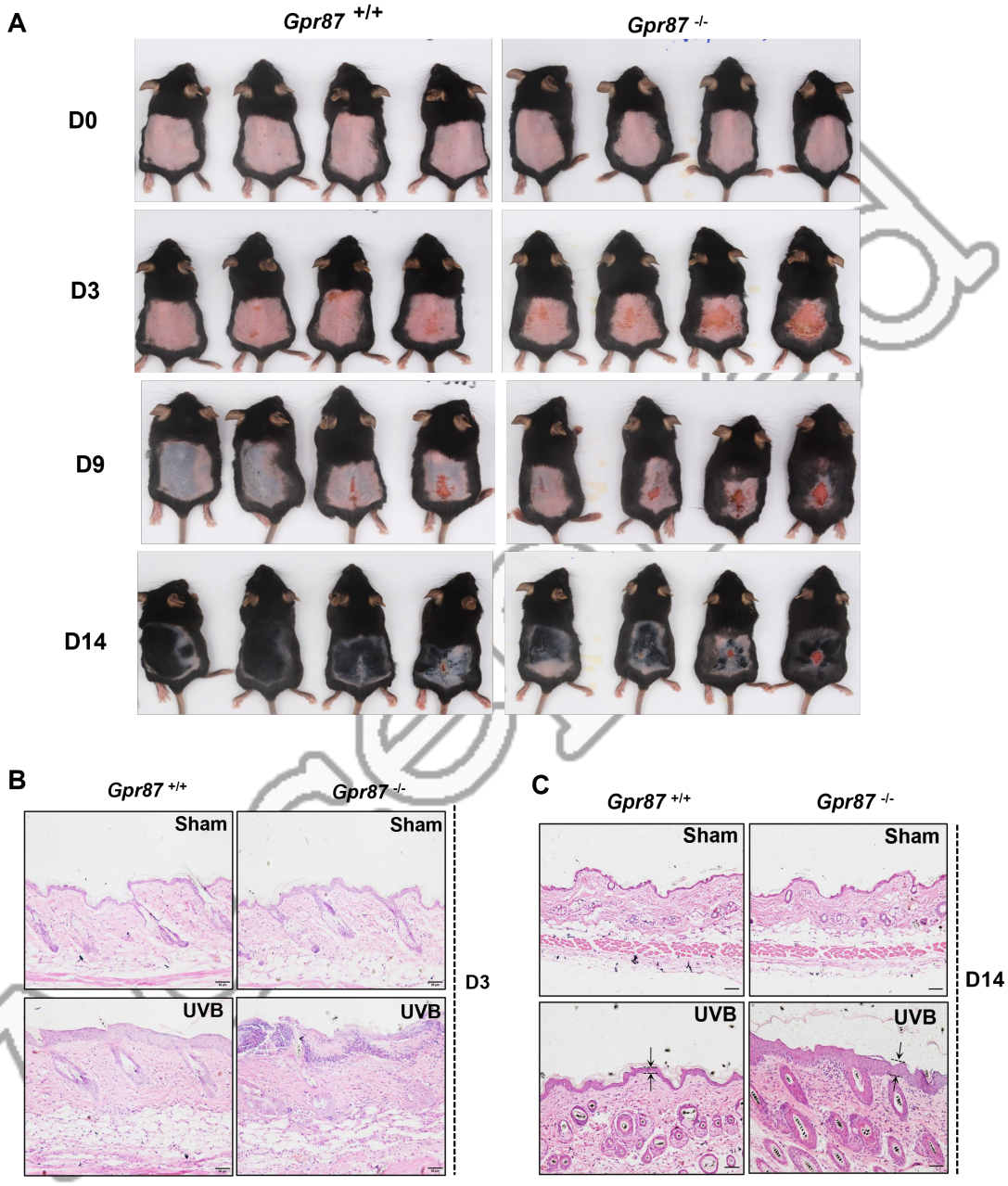

Figure 2. Gpr87 deletion exacerbates UVB induced acute skin injury in mice

A. Photographs of dorsal skin injury in *Gpr87*$^{+/+}$ and *Gpr87*$^{-/-}$ mice at 0, 3, 9 and 14 days after UVB irradiation. **B&C.** Representative H&E-staining images of dorsal skin from *Gpr87*$^{+/+}$ and *Gpr87*$^{-/-}$ mice after 3 (B) and 14 days (C) after UVB irradiation. Scale bar=50μm.

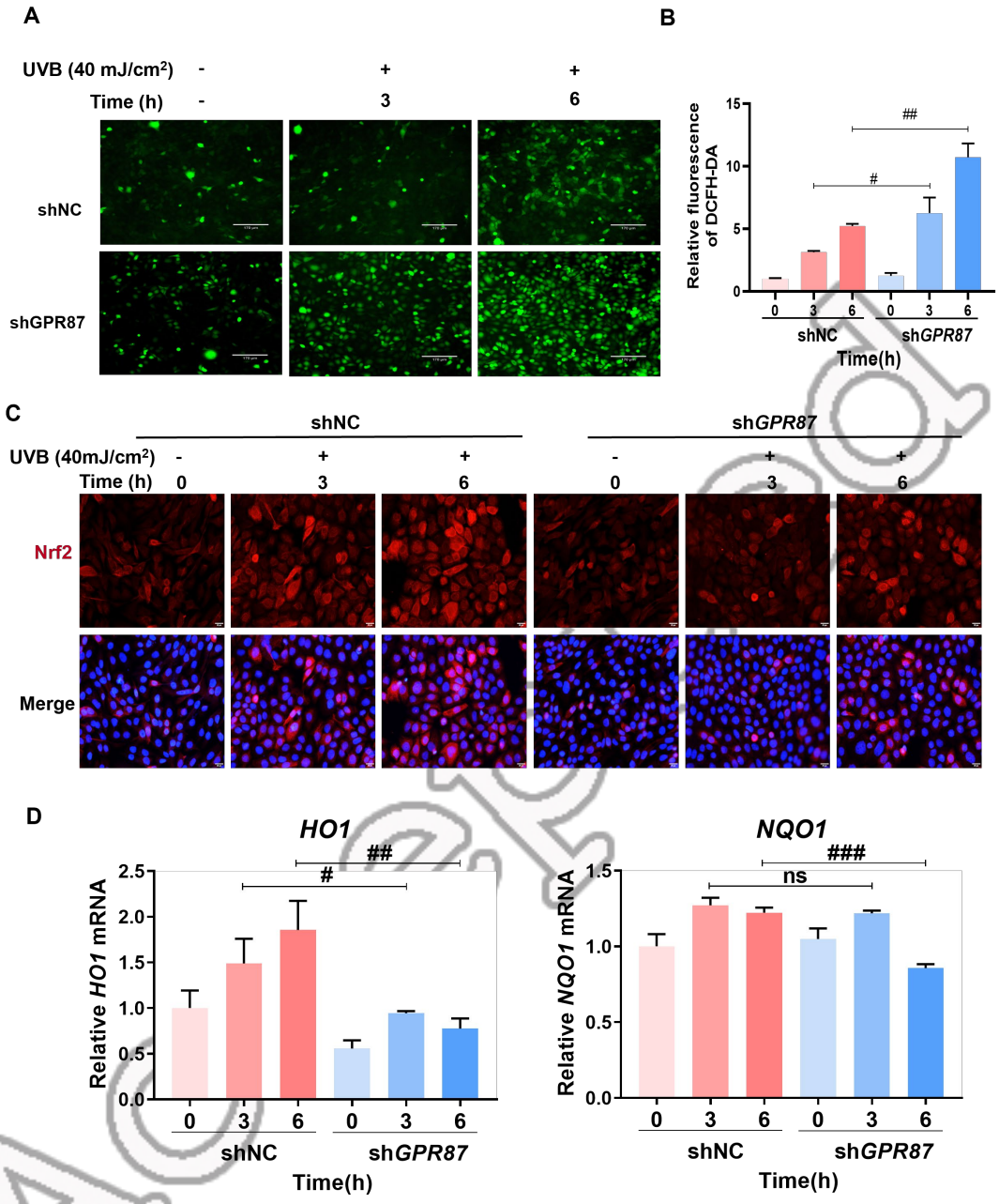

Figure 3. GPR87 deficiency elevates UVB induced oxidative stress

A. DCFH-DA fluorescent probe assay was used to measure intracellular ROS levels in shNC and sh*GPR87* HaCaT cells at 3 and 6 hours after UVB irradiation. SH, short hairpin; NC, negative control. Scale Bar=170μm. **B.** Quantification of ROS content in **(A)**. **C.** Immunofluorescence analysis of Nrf2 nuclear translocation in shNC and sh*GPR87* HaCaT cells at 3 and 6 hours after UVB irradiation. Scale Bar=20μm. **D.** The mRNA levels of antioxidant proteins such as *HO-1* and *NQO-1* in shNC and sh*GPR87* HaCaT cells was determined by qPCR. Data are presented as mean±SD (n=3). $^{\#}P<0.05$, $^{\#\#}P<0.01$, and $^{\#\#\#}P<0.001$. # indicates shN vs. sh*GPR87*.

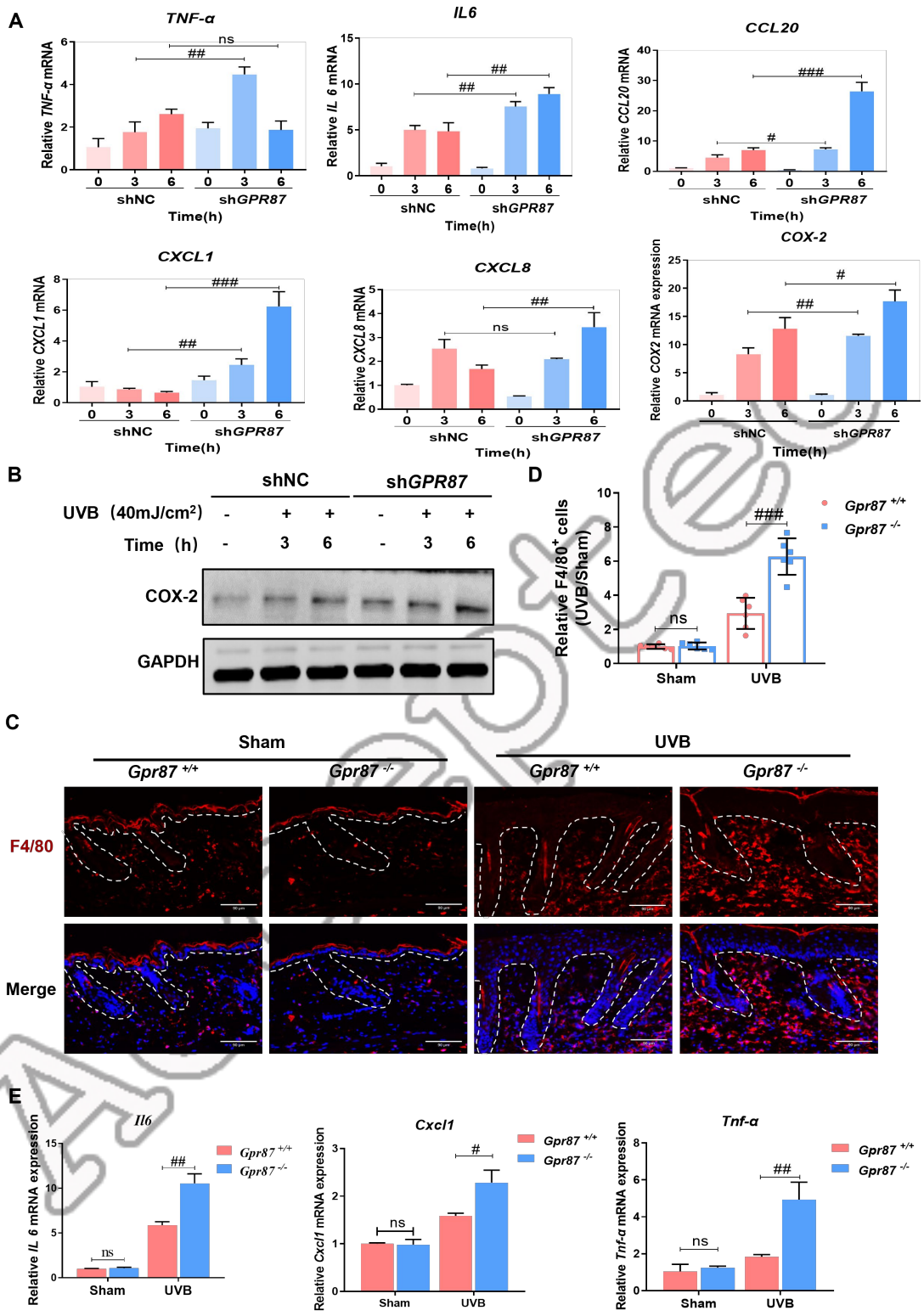

Figure 4. GPR87 deficiency aggravates UVB induced inflammatory responses

A. The mRNA levels of *IL-6*, *TNF-α*, *CXCL1*, *CXCL8*, *CCL20*, and *COX-2* in shNC and shGPR87 HaCaT cells at 3 and 6 hours after UVB irradiation was determined by RT-qPCR. **B.** The protein levels of COX-2 in shNC and sh*GPR87* HaCaT cells at 3 and

6 hours after UVB irradiation was determined by Western blot. **C.** Immunofluorescence chemistry analysis of F4/80 in dorsal skin from *Gpr87*$^{+/+}$ and *Gpr87*$^{-/-}$ mice post-UVB irradiation. Red, F4/80; blue, DAPI. Scale Bar=90 μm. **D.** Relative quantification of F4/80^{+} cell percentages compared with the UVB control group in (C). F4/80^{+}, F4/80 positive macrophages. **E**. The mRNA expression of *Il-6*, *Tnf-α* and *Cxcl1* in dorsal skin of *Gpr87*$^{+/+}$ and *Gpr87*$^{-/-}$ mice was determined by RT-qPCR. Data are presented as means±SD (n=3). $^{\#}P<0.05$, $^{\#\#}P<0.01$, and $^{\#\#\#}P<0.001$. # indicates shNC vs. sh*GPR87* (or *Gpr87*$^{+/+}$ vs. *Gpr87*$^{-/-}$).

Science Press
ZR Zoological Research

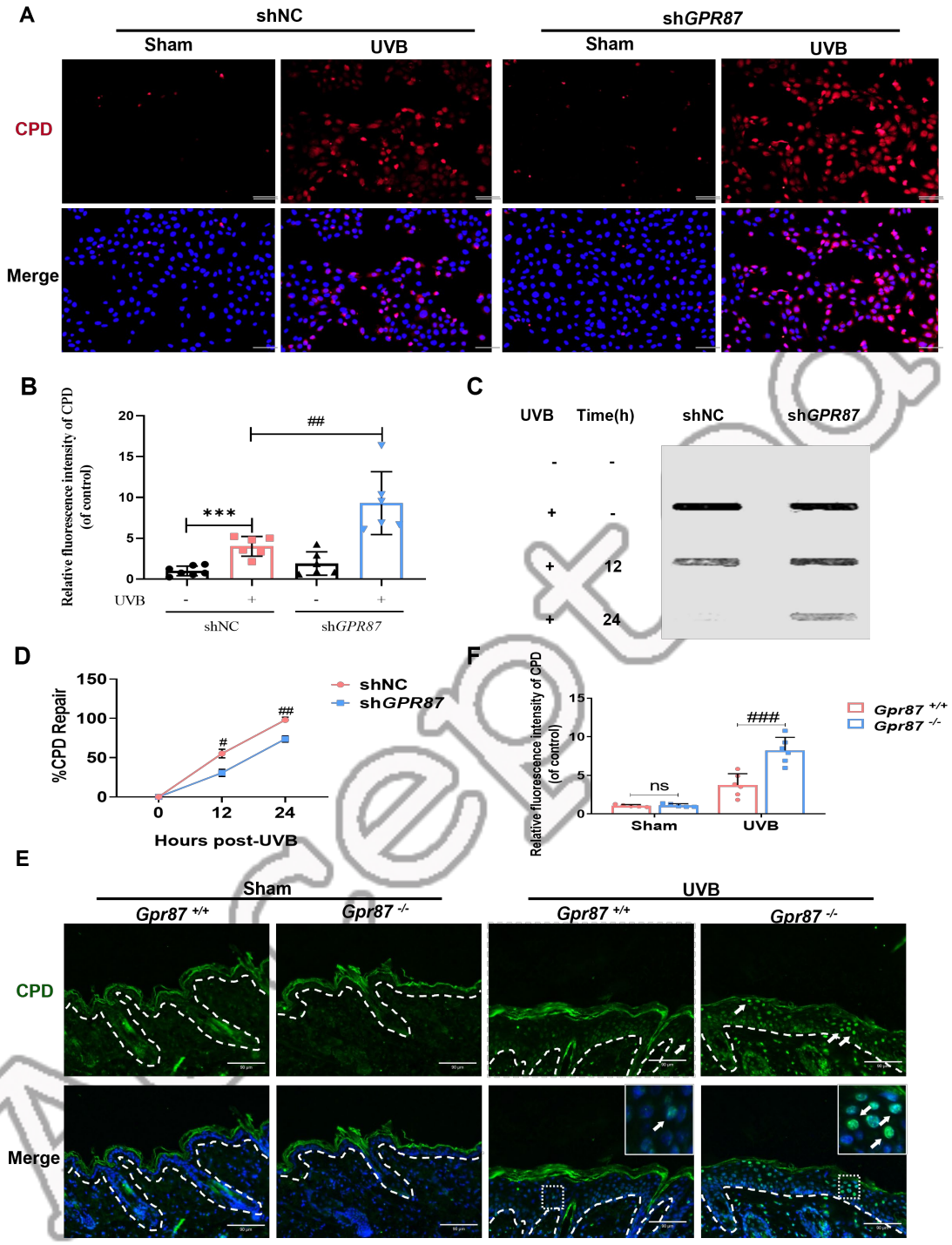

Figure 5. GPR87 deficiency increases the accumulation of UVB-induced CPDs

A. Immunofluorescence staining was performed to assess the CPD levels in shNC and sh*GPR87* HaCaT cells post-UVB irradiation. Red, CPD; blue, DAPI; CPD, Cyclobutane Pyrimidine Dimer. Scale Bar=90 μm. **B.** Quantification of fluorescence intensity of CPD levels relative to the control in (A). **(C)** Slot blot assay showing CPD levels in shNC and shGPR87 HaCaT cells at 0, 12, and 24h after UVB irradiation. **D.**

Quantification of CPD repair kinetics in (C). CPD repair rate=Relative CPD content at 12 or 24 hours after UVB irradiation/Relative CPD content at 0 hours after UVB irradiation. **E.** Immunofluorescence staining of CPD in dorsal skin sections from *Gpr87*$^{+/+}$ and *Gpr87*$^{-/-}$ mice after UVB irradiation. Scale Bar=90 μm. Green, CPD; blue, DAPI. **F.** Quantification of CPD fluorescence intensity in (E), normalized to the control. Data are presented as means±SD. (n=3). ***P<0.001; $^{\#\#}P$ <0.01 and $^{\#\#\#}P$<0.001. * indicates control vs. UVB; # indicates shNC vs. sh*GPR87* (or *Gpr87*$^{+/+}$ vs. *Gpr87*$^{-/-}$).

Science Press
ZR Zoological Research

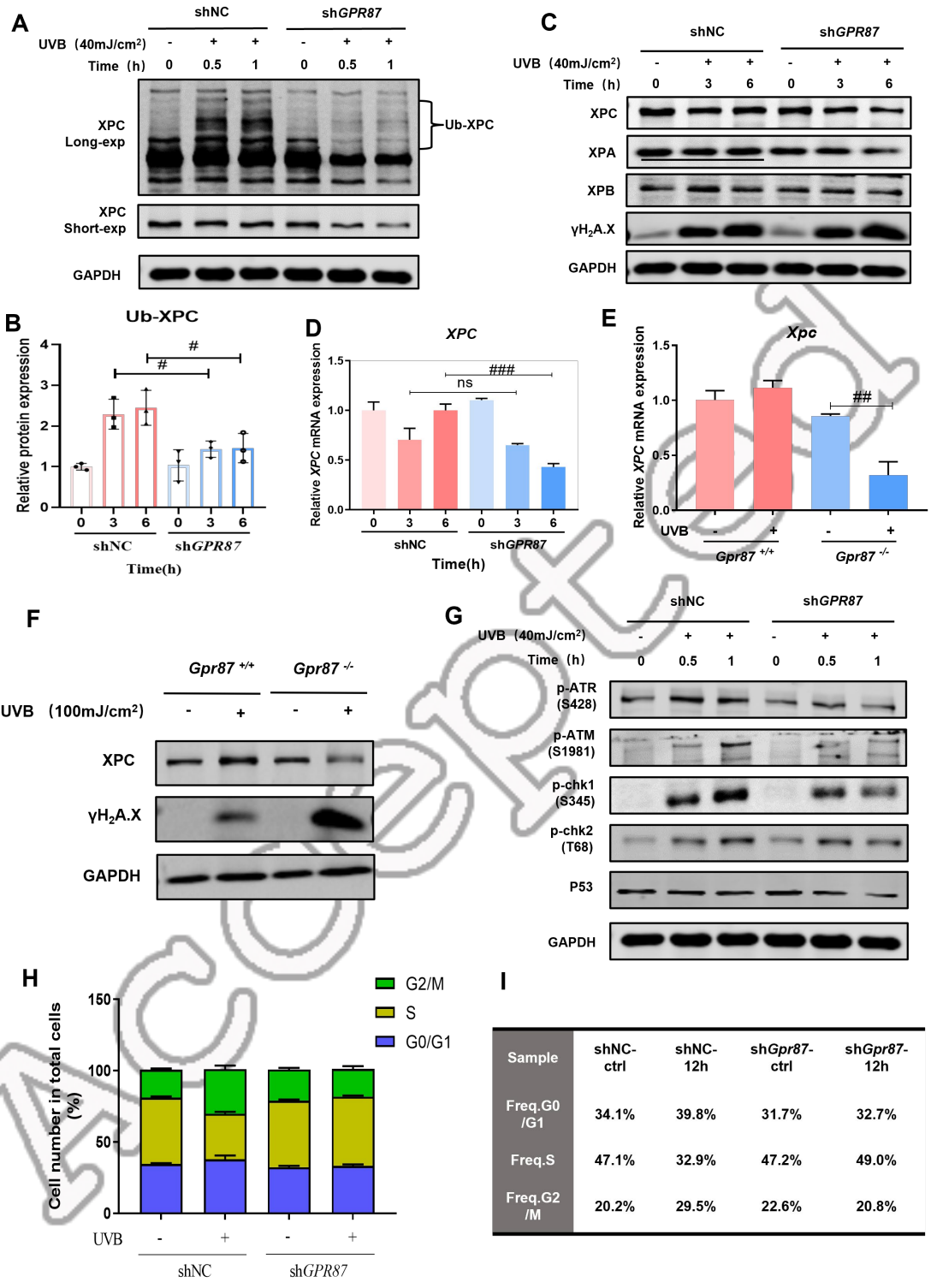

Sample	shNC-ctrl	shNC-12h	shGpr87-ctrl	shGpr87-12h
Freq.G0/G1	34.1%	39.8%	31.7%	32.7%
Freq.S	47.1%	32.9%	47.2%	49.0%
Freq.G2/M	20.2%	29.5%	22.6%	20.8%

Figure 6. GPR87 deficiency impairs the UVB induced DNA damage repair

A. Western blot analysis of XPC ubiquitination in shNC and sh*GPR87* HaCaT cells at 0, 0.5 and 1 hours after UVB irradiation. Long-exp, Long-exposure; Short-exp, Short-exposure; Ub-XPC, Ubiquitinated-XPC. **B.** Quantification of Western blot analysis of XPC ubiquitination (A). **C.** Western blot analysis of XPC, XPA, XPB and γH$_2$A.X in

shNC and sh*GPR87* HaCaT cells at 0, 3 and 6 hours after UVB irradiation. **D.** The mRNA levels of *XPC* in shNC and sh*GPR87* HaCaT cells at 0, 3 and 6 hours after UVB irradiation was determined by RT-qPCR. **E&F.** The protein levels and mRNA levels of XPC in dorsal skin of *Gpr87*$^{+/+}$ and *Gpr87* $^{-/-}$ mice post-UVB irradiation was determined by qPCR **(E)** and Western blot **(F)**. **G.** Western blot analysis of p-ATR(S428), p-ATM(S1981), p-chk1(S345), p-chk2(T68) and P53 in shNC and shGPR87 HaCaT cells at 0, 0.5 and 1 hours after UVB irradiation. **H&I.** Quantification of cell-cycle distribution (G0/G1, S, and G2/M) by flow cytometry in shNC and shGPR87 HaCaT cells after UVB irradiation. Data are presented as means±SD. (n=3). $^{\#}P$<0.05, $^{\#\#}P$<0.01, and $^{\#\#\#}P$<0.001; # indicates shNC vs. sh*GPR87* (or *Gpr87*$^{+/+}$ vs. *Gpr87*$^{-/-}$).

Science Press
ZR Zoological Research

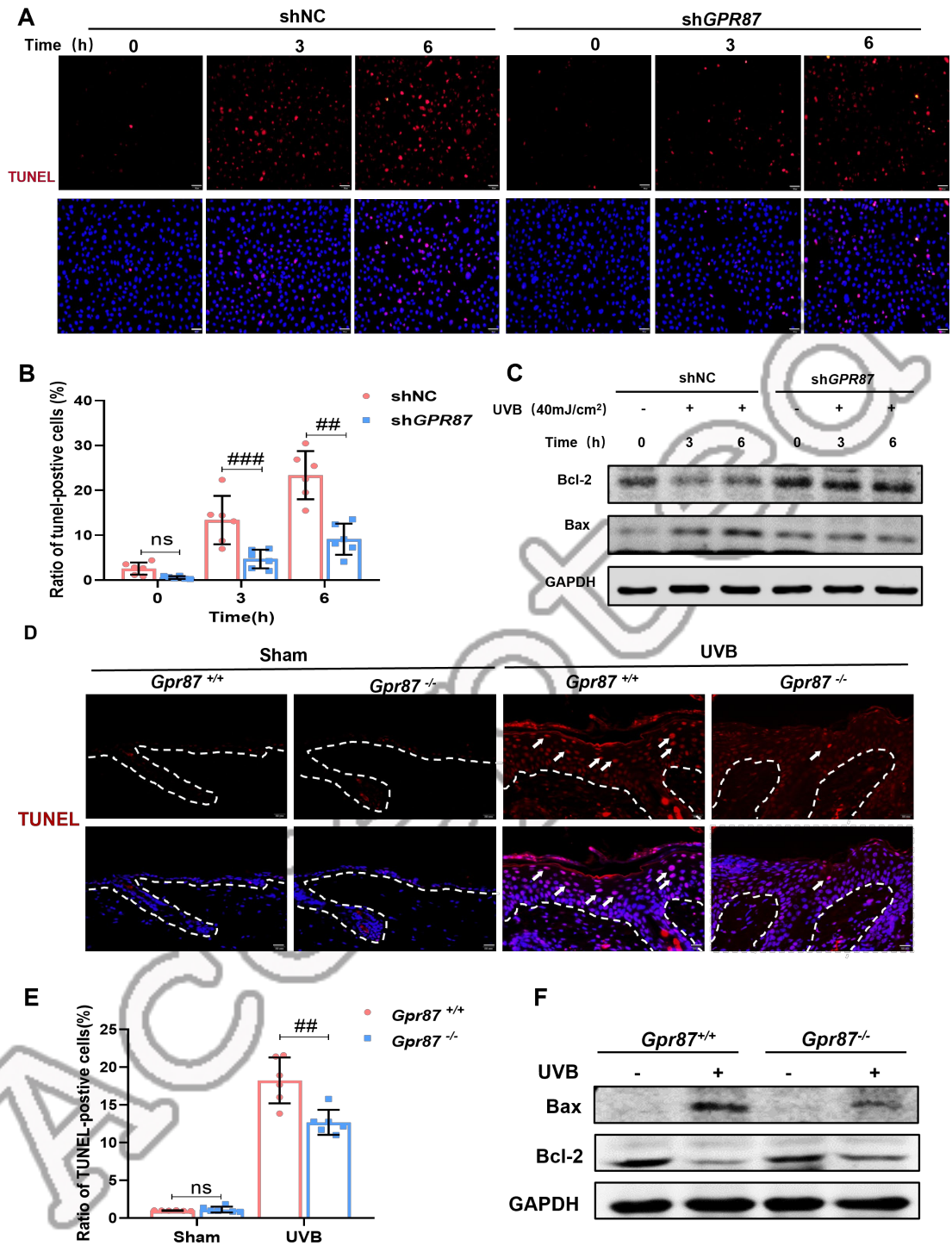

Figure 7. GPR87 deficiency inhibits apoptosis in UVB-damaged skin keratinocytes

A. TUNEL analysis of apoptosis in shNC and shGPR87 HaCaT cells at 0, 3 and 6 hours after UVB irradiation. Red, TUNEL; blue, DAPI. Scale Bar=50 μm. **B.** Quantification of ratio of apoptosis cells in (A). **C.** Western blot analysis of Bcl-2 and Bax in shNC and shGPR87 HaCaT cells at 0, 3 and 6 hours after UVB irradiation. **D.** TUNEL Assay analysis of apoptosis in dorsal skin of *Gpr87*$^{+/+}$ and *Gpr87*$^{-/-}$ mice post-UVB irradiation.

Red, TUNEL; blue, DAPI. Scale Bar=20 μm. **E.** Quantification of ratio of apoptosis cells in **(D)**. **F.** Western blot analysis of Bcl-2 and Bax in dorsal skin of *Gpr87*$^{+/+}$ and *Gpr87*$^{-/-}$ mice post-UVB irradiation. Data are presented as means±SD. (n=6). ns, not significant, $^{\#\#}P$<0.01 and $^{\#\#\#}P$<0.001; # indicates shNC vs. sh*GPR87* (or *Gpr87*$^{+/+}$ vs. *Gpr87*$^{-/-}$).

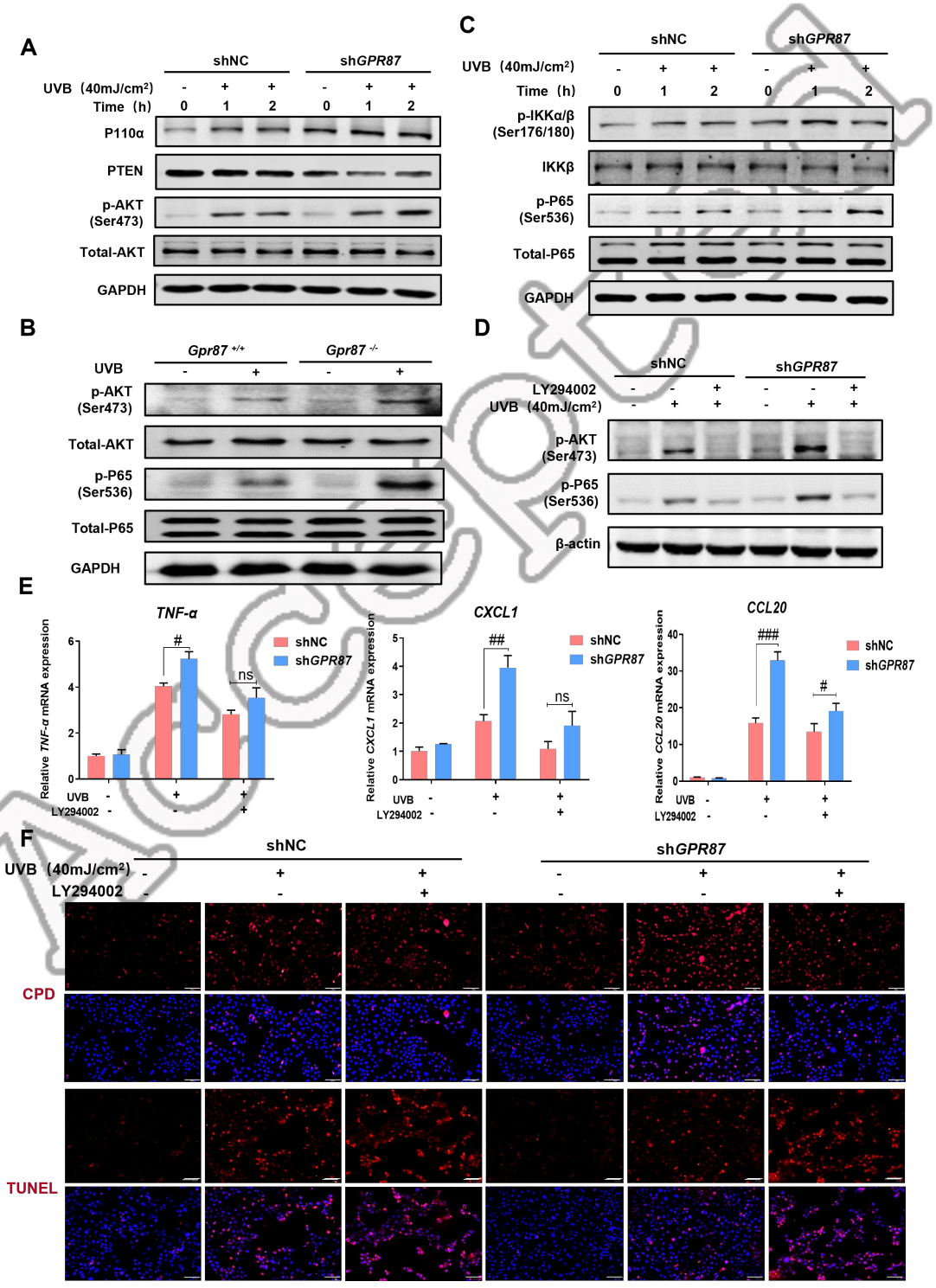

Science Press
ZR Zoological Research

Figure 8. GPR87 deficiency enhances UVB-induced skin cell damage via the PI3K/AKT pathway

A. Western blot analysis of P110α, PTEN, p-AKT (Ser473), total AKT, and GAPDH in shNC and shGPR87 HaCaT cells at 0, 1, and 2h after UVB irradiation. **B.** Western blot analysis of dorsal skin from *Gpr87*$^{+/+}$ and *Gpr87*$^{-/-}$ mice after UVB irradiation was performed to assess the PI3K/AKT and NF-κB signaling pathways by detecting p-AKT (Ser473), total AKT, p-p65 (Ser536), total p65, and GAPDH. **C.** Western blot analysiswas performed in shNC and sh*GPR87* HaCaT cells at 0, 1, and 2h after UVB irradiation to assess p-IKKα/β (Ser176/180), IKKβ, p-p65 (Ser536), total p65, and GAPDH. **D.** LY294002 (30 μmol/L) inhibited UVB-induced p-AKT (Ser473) and p-p65 (Ser536) in shNC and sh*GPR87* HaCaT cells, as shown by Western blot analysis 3h after irradiation, with β-actin as the loading control. **E.** LY294002 (30 μmol/L) suppressed UVB-induced mRNA expression of *TNF-α*, *CXCL1*, and *CCL20* in shNC and shGPR87 HaCaT cells, as determined by RT-qPCR 3h after UVB irradiation. **F.** Immunofluorescence staining was performed to assess UVB-induced CPD-positive and TUNEL-positive cells in shNC and sh*GPR87* HaCaT cells treated with or without LY294002 (30 μmol/L). Red, CPD or TUNEL; blue, DAPI; CPD, Cyclobutane Pyrimidine Dimer. Scale Bar=100μm. Data are presented as means±SD. (n=3). $^{\#}P<0.05$, $^{\#\#}P<0.01$, and $^{\#\#\#}P<0.001$; # indicates shNC vs. shGPR87 (or Gpr87$^{+/+}$ vs. Gpr87$^{-/-}$).

Science Press
ZR Zoological Research

GPR87 通过 Nrf2 和 PI3K/AKT–NF-κB 通路协调抗氧化、DNA 修复和抗炎反应，保护 UVB 损伤的皮肤

臧凯 [1#]，郭标 [1#]，于佳慧 [1]，刘若芸 [1]，刘唐霖 [1]，王财兵 [5]，许鹏 [3,4*]，党永岩 [1,2*]

[1] 华东师范大学，生物医学科学研究所与生命科学学院，上海 200241

[2] 华东师范大学，中国丽娃皮肤健康研究院，上海 200241

[3] 云南贝泰妮生物科技集团股份有限公司，昆明 650106

[4] 云南特色植物提取实验室，云南特色植物提取实验室有限公司，昆明 650106

[5] 中国科学院大学，中国科学院上海营养与健康研究所，上海 200031

[#]共同第一作者，*通讯作者，电子邮箱：yydang@bio.ecnu.edu.cn

摘要：GPR87 在多种癌症中与肿瘤发生、恶性进展及肿瘤微环境重塑相关；然而，尽管其在皮肤中高表达，其在皮肤中的功能仍很大程度上未被探索。有趣的是，我们发现 UVB 照射会下调人类皮肤组织、HaCaT 角质形成细胞及小鼠皮肤中的 GPR87 表达。此外，在 GPR87 敲除的 C57BL/6 小鼠中，GPR87 缺失加剧了 UVB 诱导的皮肤损伤。在角质形成细胞中，RNA 干扰介导的 GPR87 敲低导致活性氧（ROS）水平升高。同时，体内和体外数据均表明 GPR87 缺失增强了炎症反应和环丁烷嘧啶二聚体（CPD）积累，同时减少了皮肤细胞的凋亡。此外，GPR87 通过调节核苷酸切除修复通路关键组分 XPC 的表达与泛素化，促进 CPD 清除。机制上，GPR87 通过促进 Nrf2 核转位并诱导下游抗氧化基因表达，发挥其抗氧化作用。GPR87 缺失还会激活 PI3K/AKT 通路及其下游效应因子 NF-κB。值得注意的是，AKT 抑制剂有效逆转了 GPR87 缺失诱导的 CPD 积累和炎症反应。总之，这些发现表明 GPR87 通过 Nrf2 和 PI3K/AKT–NF-κB 通路协调抗氧化、DNA 修复和抗炎反应，保护 UVB 损伤的皮肤，从而确立定 GPR87 为环境胁迫下维持皮肤稳态的关键内源性因子。因此，靶向 GPR87 可能成为预防或减轻 UVB 诱导的光损伤及相关皮肤疾病的一种有前景的策略。

关键词：GPR87；UVB；皮肤；DNA 损伤；Nrf2；PI3K/AKT 通路

SUPPLEMENTAL INFORMATION

Supplemental Table 1. Primers used for genotyping

***Gpr87* knockout mouse genotyping prime**	**Sequence（5'-3'）**
Forward	TACACCCACCCAGAAAGAC
Reverse	AGTTGGCTGCCCATTAGTC

Supplemental Table 2. Primers used for PCR

Gene	Forward (5'-3')	Reverse (5'-3')
homo *GAPDH*	ACCCAGAAGACTGTGGATGG	TTCAGCTCAGGGATGACCTT
homo *GPR87*	GAGACGGAGCTGTTGGTAAAA	ATAGGCCCAGATTCACTGGTT
homo *HO-1*	AAGACTGCGTTCCTGCTCAAC	AAAGCCCTACAGCAACTGTCG
homo *NQO-1*	GCTGGTTTGAGCGAGTGTTC	CTGCCTTCTTACTCCGGAAGG
homo *COX-2*	TGAGCAACTATTCCAAACCAGC	GCACGTAGTCTTCGATCACTATC
homo *TNF-α*	CCTCTCTCTAATCAGCCCTCTG	GAGGACCTGGGAGTAGATGAG
homo *IL6*	GTTGTTGTTAATGGGCATTCC	GTGTCCTAACGCTCATACTTT
homo PTEN	ACCAGGACCAGAGGAAACCT	GCTAGCCTCTGGATTTGACG
homo *CXCL1*	ATTCACCCCAAGAACATCCA	CACCAGTGAGCTTCCTCCTC
homo *CXCL8*	TCTGCTAGCCAGGATCCACA	TGCTTCCACATGTCCTCACA
homo *CCL20*	TGCTGTACCAAGAGTTTGCTC	CGCACACAGACAACTTTTTCTTT
homo *XPC*	CTTCGGAGGGCGATGAAAC	TTGAGAGGTAGTAGGTGTCCAC
mus *GAPDH*	ACCCAGAAGACTGTGGATGG	TTCAGCTCAGGGATGACCTT
mus *Gpr87*	TCCGCAAACAGATGTGTTCTTA	CGCACCTCAGGATACCACTTT
mus *Il6*	AAAGAGTTGTGCAATGGCAATTCT	AAGTGCATCATCGTTGTTCATACA
mus *Cxcl1*	CTGGGATTCACCTCAAGAACATC	CAGGGTCAAGGCAAGCCTC
mus *Tnf-α*	CATCTTCTCAAAATTCGAGTGACAA	TGGGAGTAGACAAGGTACAACCC

Abbreviations: homo, Homo sapiens; mus, Mus musculus.

Science Press ZR Zoological Research

SUPPLEMENTAL MATERIALS AND METHODS

Cell viability assay

HaCaT cells were seeded in 96-well plates at a density of 1×10^4 cells per well and allowed to adhere overnight. Following UVB exposure, 10 μL of CCK-8 reagent (Dojindo) was added to each well and incubated at 37 °C for 30–60 minutes, depending on cell density. Absorbance was then measured at 450 nm using a microplate reader.

Quantitative Real-Time PCR (RT-qPCR)

Total RNA was extracted using TRIzol reagent (Invitrogen, USA), and reverse transcription was performed with the M-MLV Reverse Transcriptase Kit (Promega, USA). Quantitative PCR (qPCR) was conducted using SYBR Green Master Mix on the MX3000P system. The primer sequences were as seen as Supplemental Table 2.

Western blot analysis

Cells were seeded in 6-well plates at a density of 2×10^5 cells/mL, treated as required, and lysed in RIPA buffer. Equal amounts of protein were separated by 10% SDS-PAGE and transferred onto nitrocellulose membranes. Membranes were blocked with 5% BSA for 1 hour at room temperature, then incubated overnight at 4 °C with primary antibodies against GPR87 (Abcam, ab77517, UK), GAPDH (CST, #2188, USA), COX2 (CST, #4842, USA), XPC (CST, #12701, USA), γH2A.X(Ser139) (CST, #2577, USA), XPA (Proteintech, 16462-1-AP, China), XPB (Proteintech, 10580-1-AP, China), p-ATR (S428)(CST, #2853, USA), p-ATM(S1981) (CST, #5883, USA), p-chk1(S345) (CST, #2348, USA), p-chk2(T68) (CST, #2661, USA), p-P53(Ser15) (CST, #9284, USA), Bax (CST, #5023, USA), Bcl2 (Proteintech, 12789-1-AP, China) , Cleaved-PARP (CST, #5625, USA), P110α (CST, #4249, USA), AKT (CST, #9272, USA), p-AKT(Ser473) (CST, #9271, USA), IKKβ (CST, #8943, USA), p-IKKα/β (Ser176/180)(CST, #2694, USA), P65 (CST, #8242, USA), p-P65(Ser536) (CST, #3033, USA). After washing, fluorescently labeled secondary antibodies were applied for 2 hours at room temperature. Protein bands were detected using the Odyssey imaging system.

Hematoxylin–Eosin staining

Skin tissues were fixed in 4% paraformaldehyde, paraffin-embedded, sectioned, deparaffinized, and stained with hematoxylin and eosin (H&E) and Masson's trichrome. H&E staining was used to evaluate epidermal thickness.

Masson's trichrome staining

Masson's trichrome staining (Solarbio, Cat. G1340, China) was performed on paraffin-embedded sections following the manufacturer's protocol, in which collagen fibers stained blue, cytoplasm/muscle fibers red, and nuclei dark blue/black.

Tissue and cellular immunofluorescence

Immunofluorescence staining was performed on tissue sections or cultured cells using standard protocols. Primary antibodies against Nrf2 (Santa Cruz, #sc-365949), XPC (CST, #12701, USA), NQO-1 (Proteintech, #11451-1-AP, China), F4/80 (CST, #30325, China), CPD (Affinity, #DF9339) were incubated overnight at 4°C, followed by fluorescently labeled secondary antibodies. Images were acquired using a fluorescence microscope.

SUPPLEMENTAL FIGURE LEGENDS

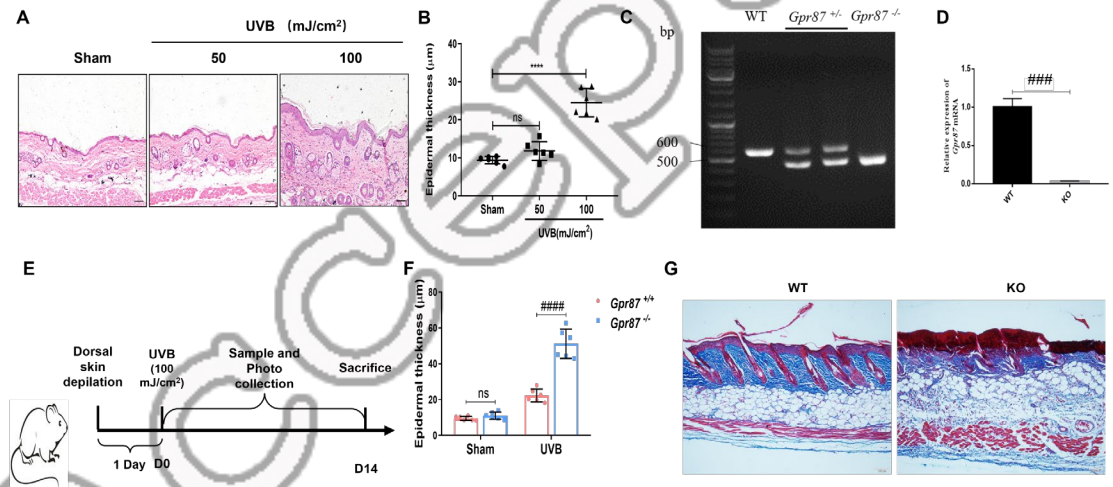

Supplemental Figure 1. Establishment of UVB-induced skin injury model in *Gpr87*$^{+/+}$ and *Gpr87*$^{-/-}$ mice. A. Epidermal changes after UVB irradiation. Depilated C57BL/6 mice were exposed to a single dorsal UVB irradiation at 50 or 100 mJ/cm². Representative H&E-stained skin sections were collected 9 days after UVB exposure. **B.** Quantification of epidermal thickness. Epidermal thickness was measured from the H&E-stained sections shown in (Supplemental Figure 1A). **C.** Genotyping PCR of mouse Gpr87 alleles. "WT" indicates wild-type mice (*Gpr87*$^{+/+}$), "*Gpr87*$^{+/-}$" heterozygous mice, and "*Gpr87*$^{-/-}$" knockout mice. **D**. qPCR analysis of Gpr87 mRNA levels in dorsal skin of wild-type and *Gpr87*$^{-/-}$ mice showing almost undetectable

expression in *Gpr87*$^{-/-}$ mice. **E**. Schematic diagram for the construction of a UVB-induced acute skin injury animal model in mice. **F**. Epidermal thickness measurements for the samples shown in Figure 1C. **G**. Masson's trichrome staining of dorsal skin of *Gpr87*$^{+/+}$ and *Gpr87* $^{-/-}$ mice after UVB exposure. Scale bar=100μm. Data are expressed as mean±SD (n=6). $^{###}P$<0.001 and $^{####}P$<0.0001, *Gpr87*$^{+/+}$ vs. *Gpr87*$^{-/-}$.

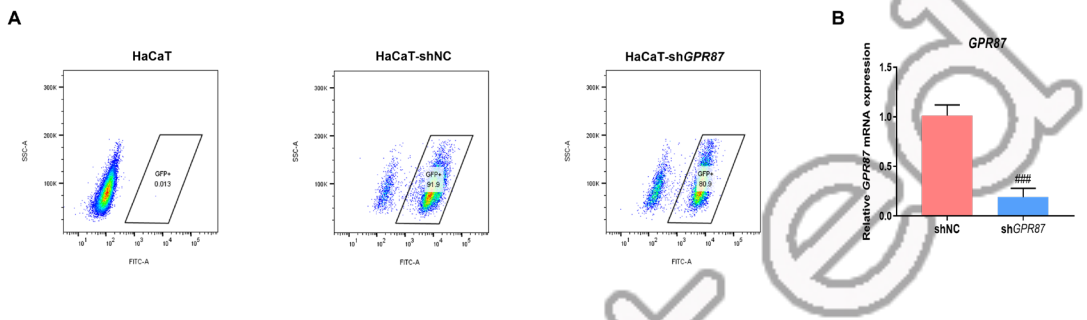

Supplemental Figure 2: **Evaluation of GPR87 knockdown efficiency in HaCaT cells**. **A**. Flow cytometric analysis of plasmid transfection efficiency. **B**. qPCR analysis of GPR87 mRNA expression. Data are expressed as means±SD. (n=3). $^{###}P$<0.001, shN vs. sh*GPR87*.

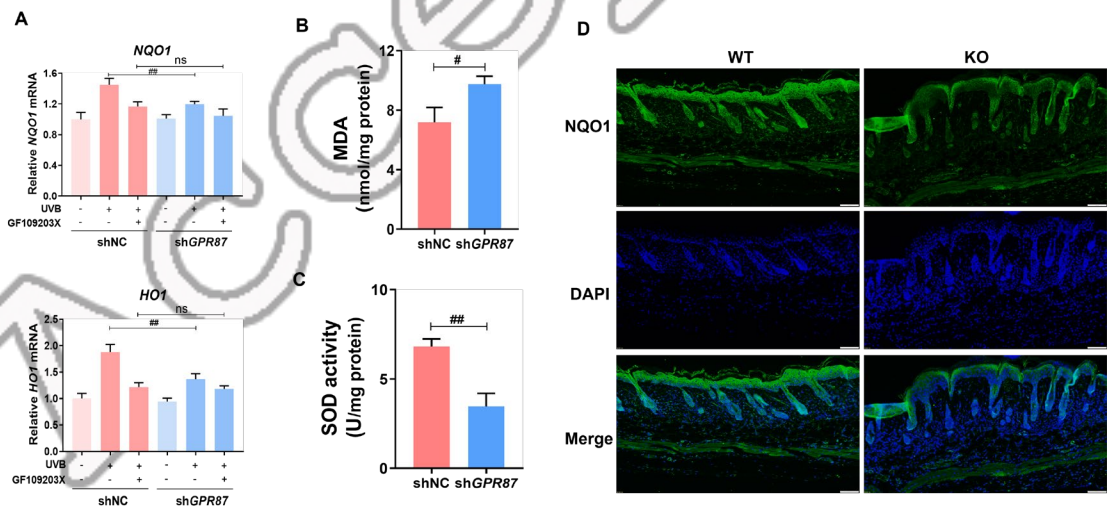

Supplemental Figure 3: **Gpr87 deficiency exacerbates UVB-induced oxidative stress.** A. **PKC inhibition attenuates GPR87-mediated Nrf2 activation**. ShN and shGPR87 HaCaT cells were pretreated with the PKC inhibitor GF109203X (2 μmol/L) for 1h, followed by UVB irradiation (40 mJ/cm²). Cells were harvested 3h after UVB exposure, and HO-1 and NQO1 mRNA levels were quantified by RT–qPCR. **B&C**. Levels of MDA (B) and SOD (C) in skin homogenates from *Gpr87*$^{+/+}$ and *Gpr87* $^{-/-}$

mice 3 days after UVB irradiation. D. Representative immunofluorescence images showing NQO1 staining in dorsal skin sections from Gpr87$^{+/+}$ and Gpr87$^{-/-}$ mice 3 days after UVB irradiation. Scale bar=100μm. Data are expressed as means±SD. (n=6). ns, not significant; $^{\#}P$<0.05, $^{\#\#}P$<0.01, *Gpr87*$^{+/+}$ vs. *Gpr87*$^{-/-}$.

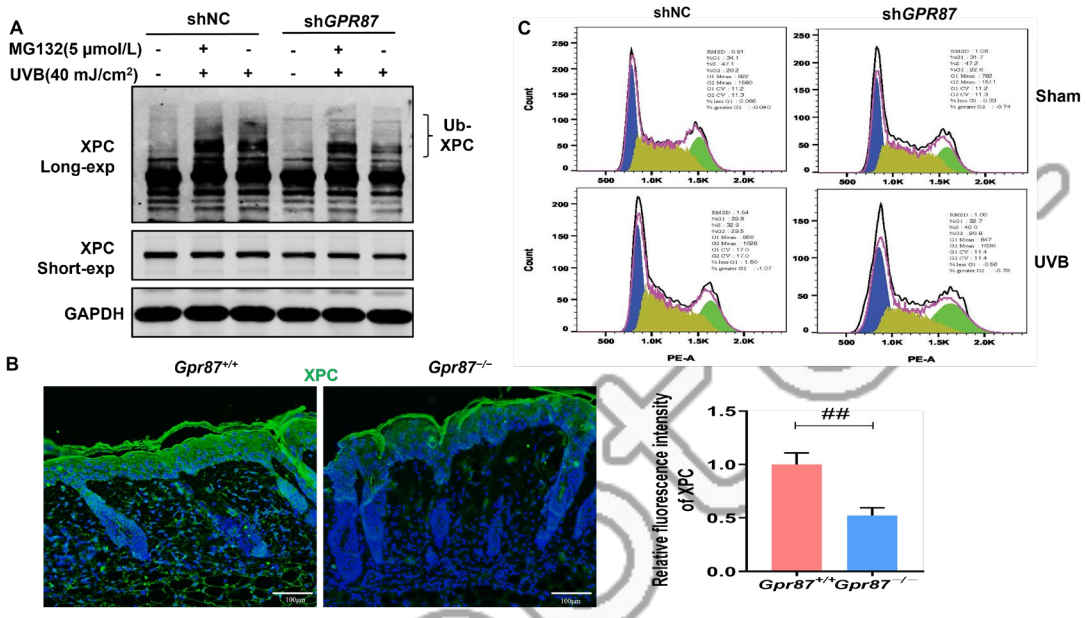

Supplemental Figure 4: **GPR87 deficiency impairs UVB-induced nucleotide excision repair of DNA damage. A**. Blocking proteasomal activity largely restored the reduced ubiquitinated XPC signal in GPR87-knockdown cells. HaCaT cells were treated with MG132 (5 μmol/L) and exposed to UVB (40 mJ/cm²) for 1h, followed by Western blot analysis. **B**. Representative immunofluorescence images of XPC staining in dorsal skin sections from *Gpr87*$^{+/+}$ and *Gpr87*$^{-/-}$ mice, and corresponding quantification, 3 days after UVB irradiation. **C**. *GPR87* knockdown altered the normal cell-cycle distribution. Flow cytometric analysis of cell-cycle phase distribution in shNC and shGPR87 HaCaT cells following UVB irradiation. Data are expressed as means±SD. (n=6) $^{\#\#}P$<0.01. *Gpr87*$^{+/+}$ vs. *Gpr87*$^{-/-}$.

Science Press
ZR Zoological Research

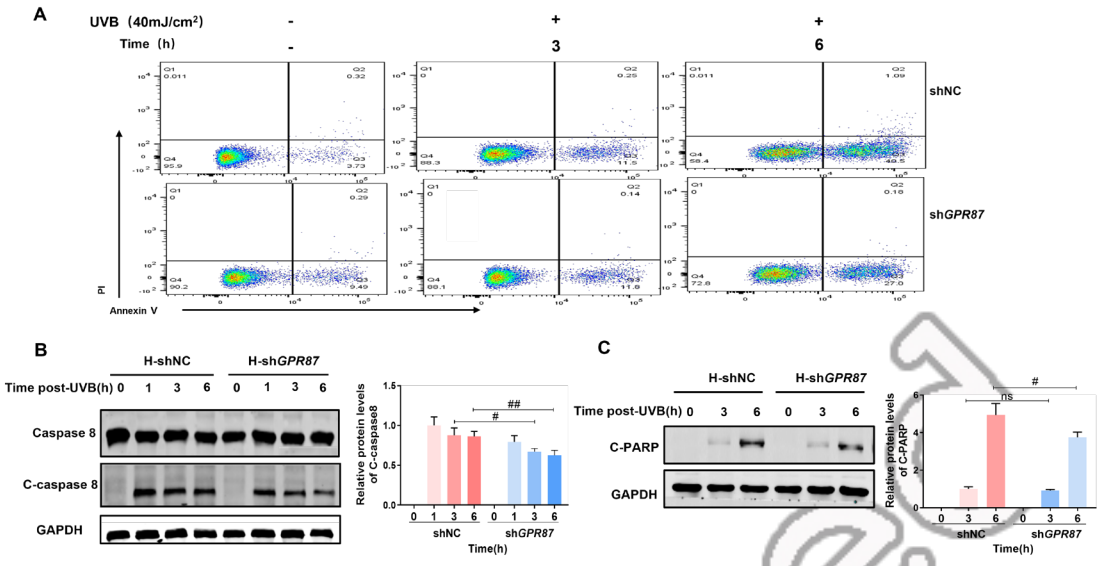

Supplemental Figure 5: **GPR87 knockdown inhibited UVB-induced apoptosis in HaCaT cells. A**. Apoptosis was assessed by flow cytometry using Annexin V/PI double staining. **B & C**. Western blot analysis of cleaved-Caspase 8 (B) and cleaved-PARP (C) with densitometric quantification in dorsal skin of Gpr87$^{+/+}$ and Gpr87$^{-/-}$ mice post-UVB irradiation. Data are expressed as means±SD. (n=3). $^{\#}P$<0.05, $^{\#\#}P$<0.01. shN vs. sh*GPR87*.

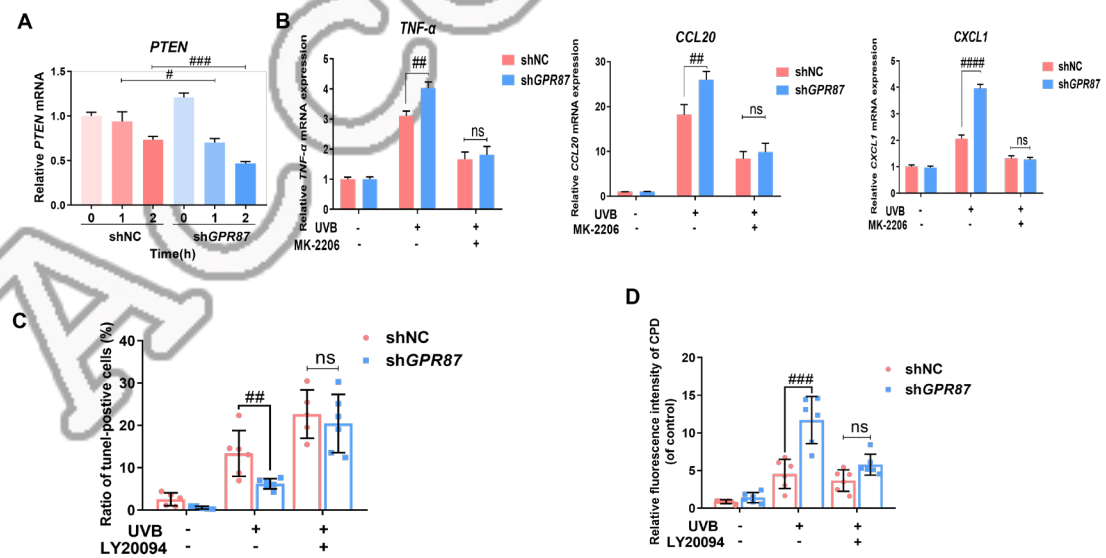

Supplemental Figure 6: GPR87 knockdown potentiates UVB-induced PI3K/AKT and NF-κB activation. **A**. RT–qPCR analysis of PTEN mRNA expression in shNC and shGPR87 HaCaT cells at 0, 1, and 2h after UVB irradiation. **B**. MK-2206 attenuates UVB-induced inflammatory gene expression in GPR87-knockdown cells. shNC and

shGPR87 cells were pretreated with MK-2206 (2 μmol/L, 1h) and exposed to UVB (40 mJ/cm²). TNFα, CCL20, and CXCL1 mRNA levels were quantified by qPCR at 3 h post-UVB. **C&D**. Quantification of CPD-positive cells (C) and TUNEL-positive cells (D) corresponding to Fig.8F. Data are expressed as means±SD. (*n*=3). ns, not significant; $^{\#}P<0.05$, $^{\#\#}P<0.01$, $^{\#\#\#}P<0.001$, shN vs. sh*GPR87*.

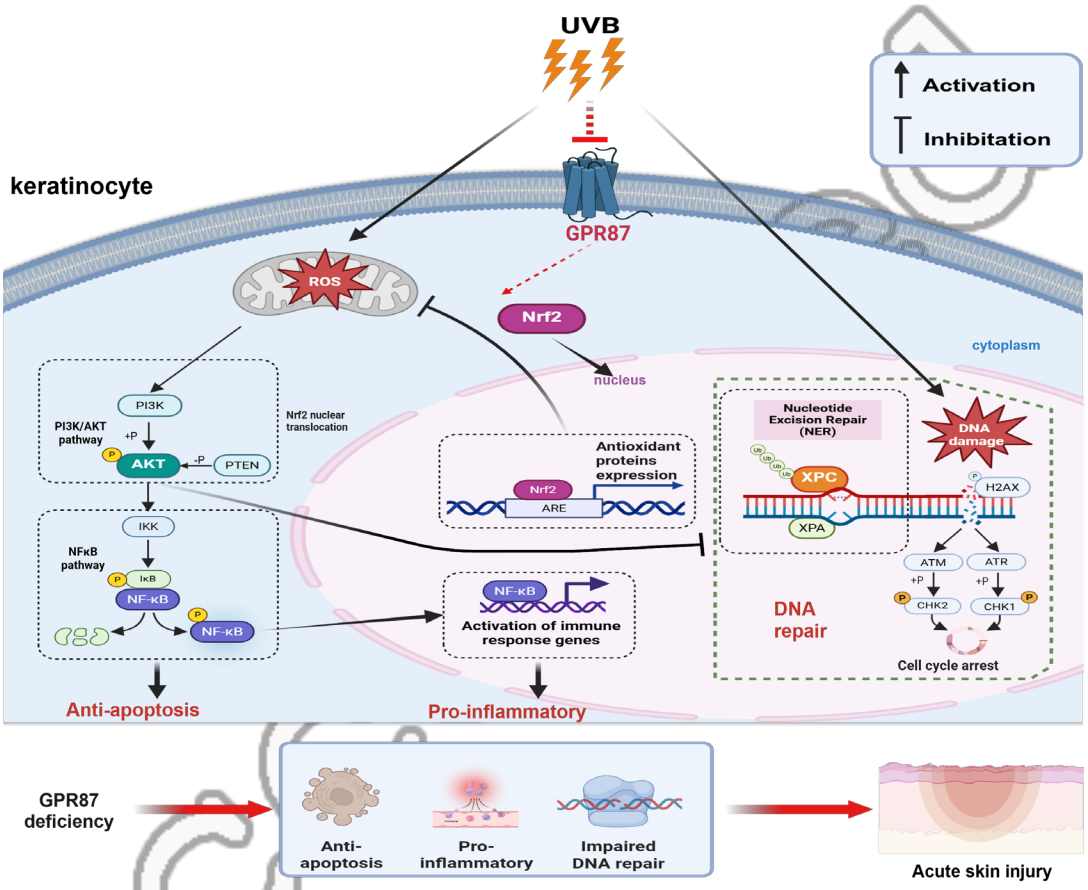

Supplemental Figure 7：A proposed model for the role of GPR87 in UVB-induced skin injury. GPR87 deficiency inhibits NRF2 activation, resulting in insufficient ROS clearance and sustained PI3K/AKT activation. Persistent PI3K/AKT activation suppresses NER factor XPC and ATM/ATR–p53 signaling, thereby impairing DNA repair and proper cell-cycle/apoptosis responses, and it further activates NF-κB to upregulate TNF-α, CXCL1, and CCL20, amplifying inflammation. Thus, GPR87 protects against UVB-induced skin injury by coordinating NRF2 and PI3K/AKT to control oxidative stress, DNA damage repair, and inflammatory responses.